CellPress

Matter

Review

Strategies for body-conformable electronics

Siyi Liu,[1] Yifan Rao,[1] Hongwoo Jang,[2] Philip Tan,[3] and Nanshu Lu[1,2,3,4,5,6,*]

SUMMARY

Advances in flexible and stretchable electronics have enabled an unprecedented level of coupling between electronics and bio-tissues by overcoming obstacles associated with the bio-tissues' curvilinearity, softness, deformability, and wetness. This review begins by detailing the outstanding challenges in achieving body-conformable electronics stemming from the disparate properties of bio-tissues and man-made materials and the complexity of their interfaces. Given tissue properties, an existing mechanics model has revealed how device softness and interfacial adhesion govern the bio-electronics conformability. Therefore, we first summarize methods for improving the mechanical compliance of electronics through both material engineering and structural design. Then, we discuss strategies to enhance bio-electronics adhesion in both dry and wet environments. We point out that innovative bio-electronics integration procedures also have a significant impact on bio-electronics conformability. We conclude by providing an outlook into future opportunities and proposing a holistic approach to strategizing body-conformable electronics.

INTRODUCTION

In the past decade, an explosion in bio-integrated electronics has advanced fields such as wearable and implantable electronics, point-of-care devices, and human-machine interfaces (HMIs).[1] Compared with conventional rigid and planar electronics, flexible and stretchable electronics possess unique advantages for bio-integration, including mechanical robustness of the devices, conformable contact or 3D coupling with bio-tissues, reduced mechanical disturbance to the bio-system, and long-term bio-compatibility. In this review, we solely focus on body-conformable electronics, a subset of bio-integrated electronics aimed at integrating planar electronics with curvilinear bio-surfaces. Figure 1 offers an ensemble of representative body-conformable electronics, including electrophysiological sensors (e.g., devices for electroencephalography [EEG], electrocardiography [ECG], electromyography [EMG], etc.),[2–6] mechanical transducers (e.g., for strain, pulse, and motion),[7] chemical bio-marker monitors (e.g., contact lens for glucose sensing, multimodal sweat-sensing wristband, etc.),[8,9] power units (e.g., energy harvesters, charging coils),[10,11] neural stimulators (e.g., e-dura, μ-LED for optogenetics),[12,13] and prostheses (e.g., artificial retina, skin protheses).[14,15] Regardless of the application, an intimate, reliable, and unobstructive bio-electronics interface is crucial for device performance and medical outcomes. For example, both experiments and theoretical models have confirmed that higher conformability leads to lower contact impedance and, ultimately, higher signal-to-noise ratios (SNRs) in electrophysiology.[16,17] Moreover, poor contact allows for relative motion at the bio-electronics interface, generating random impedance changes and even triboelectric charges under deformation.[18] Such motion artifacts could result in useless data or, even worse, misinterpretations

Progress and potential

Unobstructive, long-term, and high-fidelity human body sensing and stimulation must overcome the challenges of manifold mismatches between bio-tissues and man-made materials. The emergence of body-conformable electronics is a promising solution to these inherent obstacles. In the last two decades, various strategies have been developed to promote bio-electronics conformability by (1) improving device thinness and compliance, (2) enhancing bio-electronics interfacial adhesion, and (3) refining the bio-integration process. A successful body-conformable electronic device can only be created through comprehensive consideration of all three aspects. This review summarizes recent advancements in these three directions and proposes a holistic strategy. We envision that future research efforts in body-conformable electronics will focus on new functionalities, enhanced performance, and personalization. The rapid progress in body-conformable electronics shall meet the ever-growing demands in telemedicine, mobile health, points of care, and human-machine interfaces.

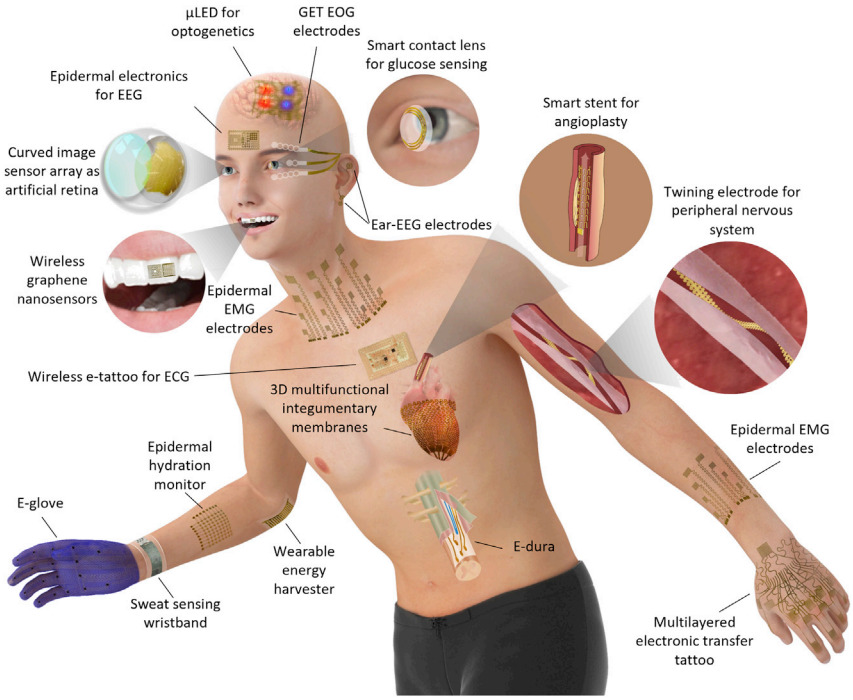


Figure 1. An ensemble of representative body-conformable electronics

Representative body-conformable electronics, including μLED conformed to the brain for optogenetics;[13] epidermal electronics for EEG;[5] curved image sensor array as artificial retina;[14] wireless graphene nanosensors integrated on the teeth for bacteria detection;[23] wireless e-tattoo for ECG;[24] large-area, multichannel epidermal EMG electrodes;[4] multifunctional e-glove;[7] epidermal hydration monitor;[25] sweat-sensing wristband;[9] 3D multifunctional integumentary cardiac membranes;[26] wearable energy harvester mounted on the elbow;[11] imperceptible GET EOG electrodes;[27] smart contact lens for non-invasive glucose sensing;[8] ear EEG electrodes;[2] e-dura over the spinal cord;[12] smart stent for angioplasty;[28] twining electrode for peripheral nerve sensing and stimulation;[29] and multilayered electronic-transfer tattoo.[30]

and is a long-standing obstacle in wearable and implantable sensors.[19] In addition to electrophysiology, conformability is also necessary for effective light, heat, or mass (e.g., sweat uptake or drug delivery) transfer across the bio-electronics interfaces, which are crucial for both bio-sensing and bio-stimulation. Therefore, the conformability of bio-electronics is a vital topic that requires broad attention and careful investigation. This topic has been touched upon in several recent reviews related to bio-integrated electronics.[20–22] However, as the majority of these reviews focused on the materials and functionalities of the electronics, there still lacks a systematic and dedicated discussion on how to achieve body conformability.

Achieving body conformability is a challenging task given the disparate mechanical properties of the human body (i.e., curvilinear, soft, deformable, and wet) and conventional electronics (i.e., planar, rigid, brittle, and dry). To provide a comprehensive overview and comparison between the two, Figure 2 offers a quantitative summary of the characteristic sizes (Figure 2A), Young's moduli (Figure 2B), strain ranges (Figure 2C), and adhesions (Figure 2D) that are pertinent to the discussions of body-conformable electronics.

Figure 2A plots the sizes and root-mean-square (RMS) surface roughnesses of various human organs, which are related to global and local curvatures, respectively. These curvatures dictate how much soft electronics need to bend and even stretch to

[1]Center for Mechanics of Solids, Structures and Materials, Department of Aerospace Engineering and Engineering Mechanics, The University of Texas at Austin, Austin, TX 78712, USA

[2]Texas Materials Institute, The University of Texas at Austin, Austin, TX 78712, USA

[3]Department of Electrical and Computer Engineering, The University of Texas at Austin, Austin, TX 78712, USA

[4]Department of Biomedical Engineering, The University of Texas at Austin, Austin, TX 78712, USA

[5]Department of Mechanical Engineering, The University of Texas at Austin, Austin, TX 78712, USA

[6]Wireless Networking and Communications Group, The University of Texas at Austin, Austin, TX 78712, USA

*Correspondence: nanshulu@utexas.edu

https://doi.org/10.1016/j.matt.2022.02.006

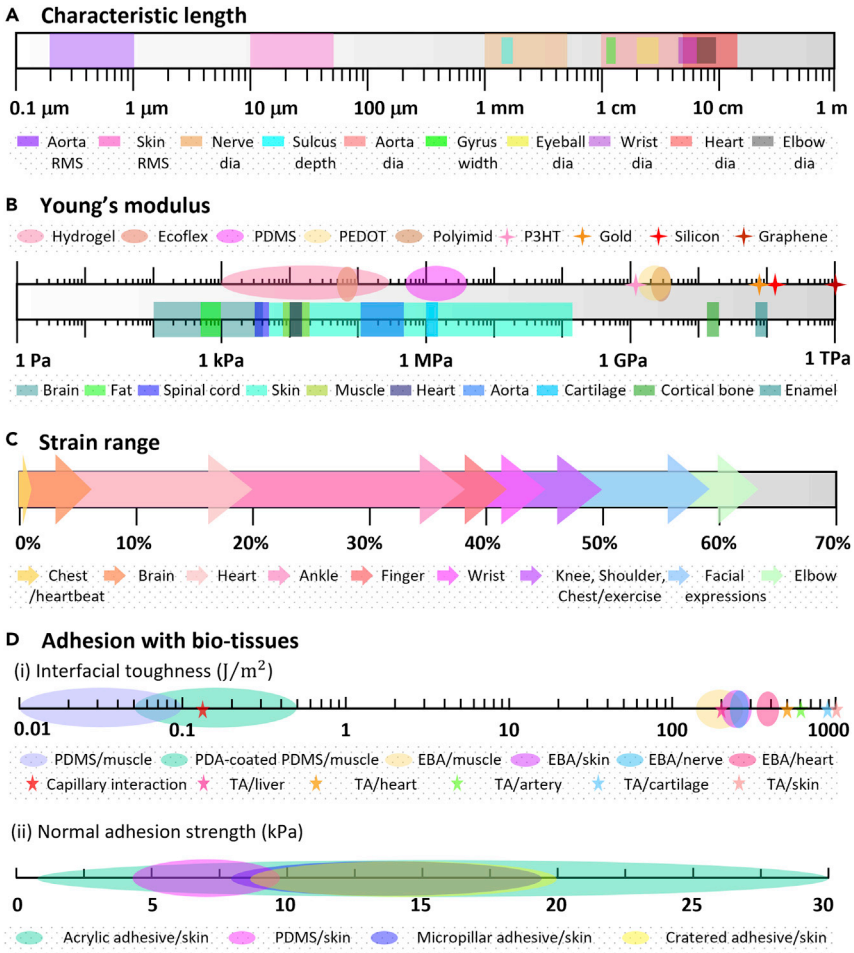


Figure 2. A quantitative summary of characteristic properties of bio-tissues, man-made electronic materials, and their interface adhesions

(A) Characteristic sizes and roughnesses of various human organs and tissues (dia refers to diameter).

(B) Young's moduli of representative man-made materials (top) and tissues (bottom).

(C) Strain ranges of different parts of the human body.

(D) Reported interfacial toughness (i) and normal adhesive strength (ii) between representative substrate materials and human tissues. PDA, polydopamine; EBA, electrical bio-adhesive; TA, slug-inspired tough adhesive.

fully wrap around or conform to the bio-tissues. Sizes of human organs range broadly. For example, the diameters of the aorta, eyeball, and heart are 1–5,[31] 2–3,[32] and 5–14 cm,[33] respectively. In addition to a wide range of organ sizes, bio-tissues also have diverse surface textures. For instance, the surface of the aorta is smooth, with an RMS roughness of only 0.2–1 μm,[34] while the RMS roughness of skin varies significantly from 10–50 μm.[35] Photos of various bio-integrated electronics in Figure 3 provide concrete examples of the various sizes of the bio-surfaces and how electronics are integrated on them. Figure 3A displays a flexible wristband for non-invasive and continuous sweat bio-marker sensing, which can bend around a wrist with a diameter of 6 cm.[9] Figure 3B is a micro-graph of 2.7-μm-thick serpentine-shaped gold-on-polyimide electrodes conforming well to the microscopic ridges of a human skin replica.[36] Intuitively, the geometric features of the target bio-tissue are a key variable to consider when designing body-conformable electronics.

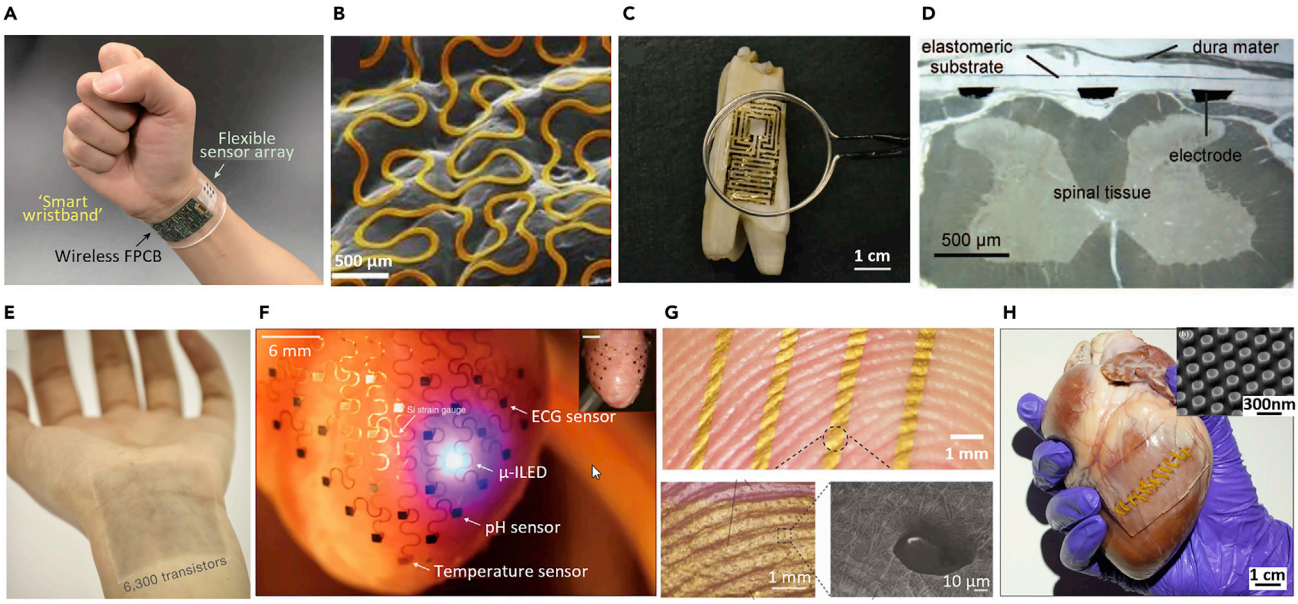


Figure 3. Experimental photos of various body-conformable electronics as example demonstrations of Figure 2

(A) A smart wristband capable of non-invasive, continuous, and wireless sweat sensing of five different bio-markers.[9]

(B) Epidermal electrodes with fractal serpentine design well conformed to a human skin replica.[36]

(C) A flexible wireless graphene sensor on a tooth for bacteria detection.[23]

(D) An e-dura attached to the spinal cord for nerve stimulation.[12]

(E) A stretchable transistor array made out of intrinsically soft and stretchable dielectrics, semiconductors, conductors, and substrates.[37]

(F) A multifunctional integumentary electronic device with island-plus-serpentine design for epicardial monitoring.[38]

(G) Gas-permeable, stretchable, ultrathin, and skin-conformable electrodes made out of gold nanomeshes.[39]

(H) An elastomer substrate with nanosucker array (inset) for enhanced adhesion on a porcine heart.[40]

Figure 2B lower axis exhibits the wide range of Young's moduli of different human tissues (100 Pa of cerebral tissue to 10 GPa of bones), a topic already widely covered in other reviews.[21,41–43] Since popular inorganic and even organic electronic materials (upper axis) are much stiffer than most bio-tissues, typical electronics are ill-suited for interfacing with the body. For example, gold, silicon, poly(3,4-ethylenedioxythiophene) polystyrene sulfonate (PEDOT:PSS), and poly(3-hexylthiophene-2,5-diyl) (P3HT) have moduli of 79, 140, 1–2.7,[44] and 1.3 GPa,[45] respectively. Conversely, bio-tissues like the spinal cord and skin are much softer, with moduli of 3–5 kPa[46] and 5 kPa–140 MPa,[47] respectively. Such a significant stiffness mismatch may impose either a large constraint to the natural motion of the bio-tissues (e.g., an integumentary sensor over the heart restricting cardiac relaxation during diastole) or a large distortion in the bio-tissues (e.g., a silicon-based artificial retina flattening the actual retina). Even worse, the stiffness of the electronics can cause tissue damage, such as heart-rate-monitoring chest straps chafing the skin or silicon-shank-based brain probes causing neuron damage.[48] Generally speaking, it is advantageous to minimize the stiffness mismatch. For instance, since teeth are very stiff, a graphene-based, non-stretchable sensor is acceptable (Figure 3C);[23] conversely, an e-dura wrapping around extremely soft spinal tissue requires a much softer elastomeric substrate (Figure 3D).[12,49] Therefore, bio-tissue stiffness is another essential factor to be accounted for when engineering body-conformable electronics.

In addition to characteristic size and softness, the continuous deformation of bio-tissues is a prominent issue for bio-electronics, as summarized in Figure 2C. For example, joint movements can deform the skin by more than 60%,[50,51] heartbeats

can lead to cardiomyocyte deformation by 20%,[52] and even the brain deforms by 6% under mild angular head impact.[53] However, inorganic materials used in conventional electronics (e.g., copper, silicon, etc.) have a yield or rupture strain smaller than 1%. As body-conformable electronics must not fail mechanically (either internally or interfacially) by the deformation of the underlying tissue nor pose a mechanical constraint to the natural motion of the tissue, substantial research has been conducted to develop stretchable and compliant conductive and semiconducting materials, such as liquid metal, conductive hydrogel, and conductive/semiconducting polymers.[37,54–57] For example, Figure 3E illustrates a stretchable transistor array composed of intrinsically soft materials, including polymeric dielectrics, semiconductors, conductors, and the substrate.[37] Another approach is to engineer the geometry of intrinsically stiff materials into more compliant structures through patterning and/or buckling, such as serpentine and kirigami patterns and buckled structures.[57,58] Figure 3F displays a soft integumentary epicardial monitor employing the island-plus-serpentine design to incorporate stiff μ-LEDs and electrode pads, which can survive the strain induced from heartbeats while applying an imperceptible constraint to cardiac motion.[38] Clearly, the mechanical deformation of bio-tissues is one more important consideration for body-conformable electronics.

Conformability to bio-tissues also depends on the bio-electronics' interfacial adhesions, which are usually quantified through interfacial toughness (J/m^2) or adhesive strengths (kPa), as summarized in Figures 2Di and 2Dii, respectively. The interfacial toughness indicates the amount of energy required to cause detachment. The normal or shear adhesive strength denotes the required maximum tensile or shear stress to separate the two contacting surfaces. Without additional adhesives, adhesion based solely on van der Waals or capillary (0.144 J/m^2) interactions between man-made materials and bio-tissues is very weak. For example, silicone elastomers such as polydimethylsiloxane (PDMS) are widely used as the substrate and encapsulation material for body-conformable electronics due to their bio-compatibility and -stability; however, the adhesive strength between PDMS and skin is only 3–9 kPa,[59] which is 20 times smaller than that of Scotch tape (180 kPa). Despite such weak adhesion, conformability can still be achieved if the device is ultrathin, such as 500-nm-thick graphene electronic tattoos (GETs) resting on human skin[17,27] and the 100-nm-thick gold nanomesh conforming to fingerprint textures shown in Figure 3G.[39] To enable thick films to conform to bio-tissues, adhesives for both dry and wet surfaces have been engineered. Dry adhesives (or, more rigorously, physically enhanced adhesives) include gecko-inspired micro-pillar arrays[60] and cratered surfaces, which can achieve enhanced adhesive strengths up to 115 kPa compared with unstructured surfaces. Figure 3H illustrates that a PDMS surface patterned with a nanosucker array can generate sufficient adhesive forces to strongly adhere to a porcine heart.[40] Chemically engineered bio-adhesives such as acrylic and hydrogel adhesives[61,62] can achieve much higher interfacial toughnesses of up to 1000 J/m^2.[61] Detailed examples of both types of adhesives are offered and discussed later in this review. These revolutionary advances in bio-compatible adhesives have made a significant impact on body-conformable electronics.

Finally, the process of applying electronics to bio-surfaces is a complex topic, especially because soft electronics are more difficult to handle and manipulate as they become so floppy. Other complications, such as large area coverage and tissue breathability, also necessitate the development of novel bio-integration methods.

Based on the above-listed motivations, we summarize strategies to achieve body-conformable electronics in this review from the following three aspects. First, we

outline state-of-the-art material engineering and structure designs to make electronics compatible with the softness and deformability of bio-tissues. Second, we review recent progress in bio-electronic interface adhesives under both dry and wet conditions. Third, a variety of emerging bio-integration methods are summarized. Toward the end, we discuss the remaining challenges and promising solutions in body-conformable electronics. Finally, we offer a holistic perspective for engineering body-conformable electronics.

CONFORMABILITY MODEL AND EXAMPLES

Experiments have shown that conformal contact between the tissue surfaces and the electronic devices can be affected by various mechanical properties, including tissue and device stiffness, tissue surface curvature and roughness, device thickness, interfacial adhesive strength, and deformation.[16,17,39,63] Therefore, it is vital to have mechanics models that consider those variables and offer quantitative guidelines for properly optimizing those parameters. Several theoretical models have been developed for this purpose.[64–66] The basic ideas are introduced here.

Flexible but inextensible electronics are only able to conform to surfaces with zero Gaussian curvatures, such as cylindrical surfaces and other two-dimensional (2D) wavy surfaces with zero curvature in the third dimension. In general, brittle components are placed on the neutral axis in these types of flexible electronics. For a multilayer system where an enormous mismatch of modulus exists between layers, the conventional Euler-Bernoulli beam theory breaks down. Instead, a split of the neutral axis occurs, which means multiple neutral axes can co-exist inside a multilayer system.[67] The location of the neutral axes may shift depending on the bending curvature, so practical implementation is not as straightforward as what can be modeled with Euler-Bernoulli beams.[68] It is possible to conform inextensible electronics to 3D-curvilinear surfaces if cuts in the 2D electronic sheet are permitted.[14] Computational methods to design such cuts are still being explored and will be discussed further in the outlook section.

The large tensile stiffness of flexible but inextensible electronics makes them undesirable for soft-tissue integration due to the dynamic motion of those organs, as summarized in Figure 2C. Therefore, compared with solely flexible electronics, stretchable electronics are much more widely used in body-conformable devices. Figure 4A displays a highly simplified 2D schematic of a linearly elastic thin membrane conforming to a soft substrate with wavy surface, which is used to model a stretchable thin-film device trying to conform to a rough tissue surface.[64] The substrate with infinite thickness has a plane strain Young's modulus of $\overline{E}_s$ and an undeformed sinusoidal surface with a wavelength of λ and an amplitude of h_0, representing the modulus of the tissue (representative values displayed in the lower axis in Figure 2B) and the characteristic length scale of tissue surface (Figure 2A), respectively. The thin membrane has a plane strain Young's modulus of $\overline{E}_m$ and a thickness of t, representing the modulus of device (upper axis in Figure 2B) and the thickness of device, respectively. The membrane is flat before conforming to the substrate. The membrane-substrate interfacial work of adhesion γ (Figure 2D) is the only driving force for membrane-substrate conformation, which deforms both the membrane and the substrate. x_c represents the conformed region, and its normalized form is $\widehat{x}_c = x_c/(\lambda/2)$. Three possible deformed configurations are considered: fully conformed ($\widehat{x}_c = 1$), partially conformed ($0<\widehat{x}_c<1$), and non-conformed ($\widehat{x}_c = 0$). Because energy minimization is a well-established method to determine the equilibrium configuration, we first establish the total potential energy of the system to be

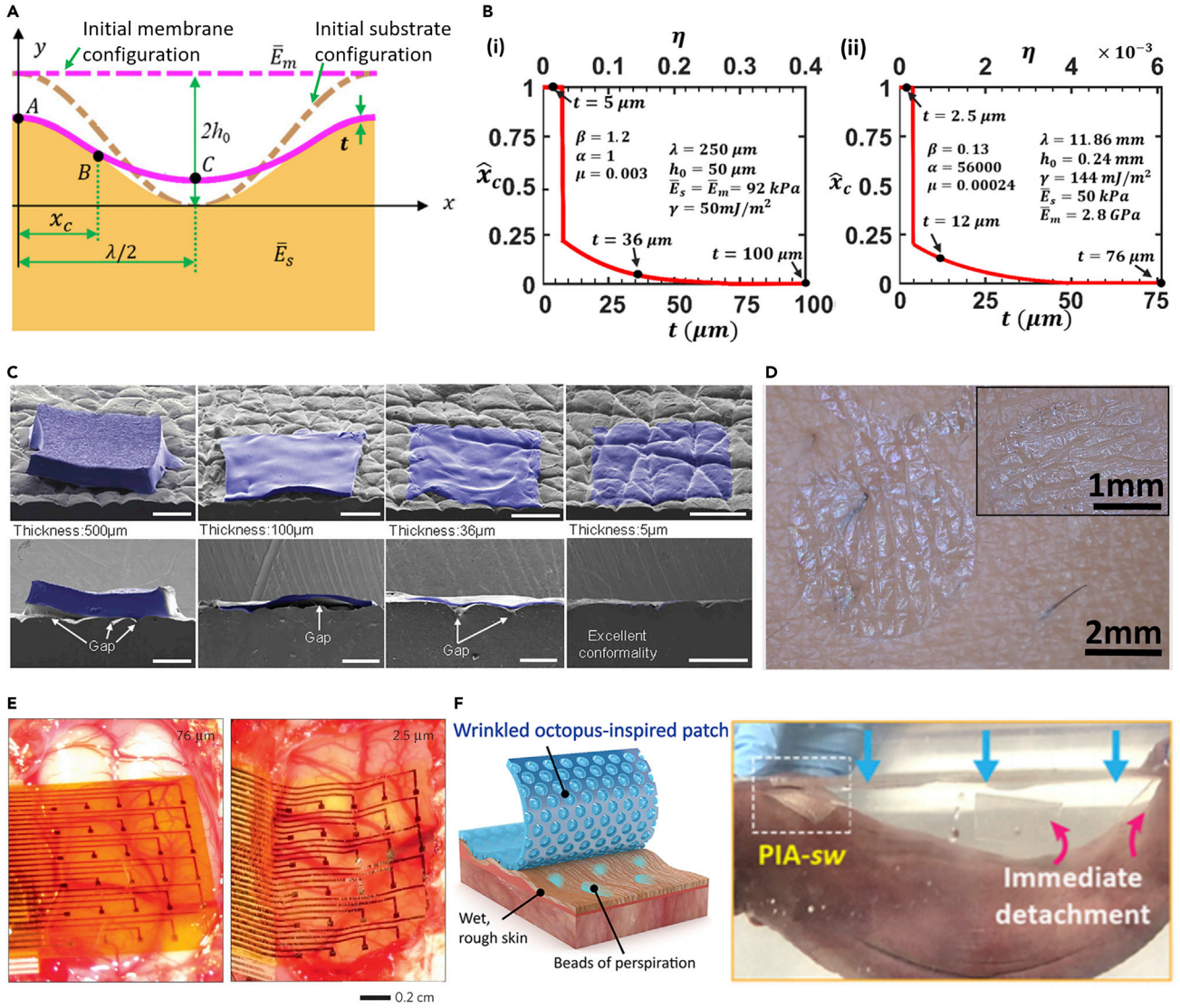


Figure 4. Conformability model and examples

(A) Schematic of a 2D conformability model and controlling parameters.[64]

(B) Theoretically predicted normalized contact zone size, i.e., conformability, as a function of film thickness for (i) an Ecoflex film on the skin and (ii) a polyimide film on the brain.[64]

(C) Experiments of an Ecoflex film with various thicknesses on a skin replica.[16]

(D) Experimental photo of a GET on the skin.[69]

(E) Experiments of a polyimide film of two different thicknesses on a feline brain.[63]

(F) Schematic of a nanosucker enabled adhesive (left panel). It stays well attached on a porcine liver underwater (yellow label), whereas an unpatterned substrate demonstrates immediate detachment from the liver (white label) (right panel).[70]

$$\Pi = U_{bending} + U_{stretching} + U_{adhesion} + U_{substrate}, \qquad \text{(Equation 1)}$$

where $U_{bending}$ and $U_{stretching}$ represent the bending and stretching energy in the membrane, respectively, and can be expressed in terms of the bending stiffness, membrane stiffness, and strain in the membrane. $U_{substrate}$ represents the strain energy in the substrate, which is equivalent to work done to the substrate, i.e., the product of traction and displacement on the substrate surface. $U_{adhesion}$ represents the interfacial adhesion energy and can be obtained as the product of interfacial work of adhesion γ and the contact area.

After normalization, it is revealed that four dimensionless parameters, $\alpha = \overline{E}_m/\overline{E}_s$, $\beta = 2\pi h_0/\lambda$, $\eta = t/\lambda$, and $\mu = \gamma/(\overline{E}_m\lambda)$, control the energies and, ultimately, the conformability.[64] These parameters represent the membrane-to-substrate modulus ratio, the normalized roughness of the substrate, the normalized membrane thickness, and the normalized interfacial adhesion, respectively. By minimizing the total potential energy numerically, the normalized contact zone size $\hat{x}_c$ can be solved, as plotted in Figure 4B, where the membrane thickness is the only variable and the other controlling parameters are assumed constants, as labeled in the two plots. One significant conclusion is that the effect of each parameter is monotonic: the membrane tends to better conform to the rough substrate as the membrane modulus decreases, the substrate roughness reduces, the membrane thickness diminishes, or the interfacial work of adhesion increases. Furthermore, an abrupt transition from fully conformed to merely conformed ($\hat{x}_c =$ 23%) states can be observed for all four dimensionless controlling parameters due to snap-through mechanical instability.[64]

Four experiments of body-conformable electronics in the literature can be used to validate this theory. The best example is an Ecoflex membrane attached to a skin replica where only the van der Waals interaction is involved (Figure 4C).[16] From the figure, it is obvious that the 5-μm-thick Ecoflex membrane can fully conform to the skin, but 36- and 100-μm-thick ones cannot. This experimental observation is consistent with the theoretical results plotted in Figure 4Bi—the critical thickness of Ecoflex to fully conform to the skin is 7.5 μm.[64] This prediction is obtained by assuming the membrane is Ecoflex, whose plane strain Young's modulus is comparable to that of the skin (92 kPa). The stiffer the membrane, the smaller the critical thickness must be to achieve full conformability. When we consider a much stiffer membrane such as the GET, essentially a graphene on polymethyl methacrylate (PMMA) bilayer whose modulus is dominated by that of the PMMA (3.3 GPa), the theory predicts the critical thickness to be only 510 nm. Figure 4D experimentally demonstrates that a GET with a total thickness of 463 $\pm$ 30 nm is able to fully conform to the skin.[17,69] The third example is a polyimide-supported gold flexible electrode array conforming to the surface of a brain (Figure 4E),[63] which is wet, and, hence, the interface work of adhesion (0.144 J/m^2) is simply twice the surface tension of water. The experiment shows that the 76-μm-thick sample stays flat on the brain, whereas the 2.5-μm-thick sample can achieve full conformability. Figure 4Bii predicts 5 μm to be the theoretical critical thickness,[64] which again agrees with the experimental observation. In another example of conformability to a wet surface, as shown in Figure 4F,[70] an unpatterned PDMS sheet and a PDMS sheet with surface suction cups were attached to a porcine liver, but only the latter was able to stay adhered to the liver surface underwater due to the suction-cup-enhanced adhesion. The last example illustrates that enhancing interfacial adhesion is effective in improving conformability.

In summary, based on experimentally validated theoretical models, the conformability of bio-integrated electronics can be improved by (1) reducing device thickness, (2) reducing device effective stiffness, and (3) enhancing the adhesion between the electronics and the target tissue surface. In the following sections, we discuss various strategies based on these guidelines.

MATERIAL AND STRUCTURAL STRATEGIES

While reducing device thickness is straightforward (e.g., thinning down silicon die or polyimide substrate, using atomically thin 2D materials),[5] reducing the stiffness of

electronics is much more complicated. This section will focus on thin-film materials and structural designs that help reduce device effective stiffness. Here, the effective stiffness only refers to the in-plane tensile stiffness or effective modulus because the bending stiffness just scales with the product of modulus and thickness cubed. From the material perspective, intrinsically low-modulus materials such as nanocomposites, rubbery electronics, hydrogels, and liquid metal are being widely explored for stretchable electronics. From the structural perspective, meandering serpentine ribbons, mesh designs and kirigami designs offer possible geometric remedy for intrinsically stiff materials.

Material compliance

Metals and silicon are well-established electronic materials, but they are intrinsically stiff. To find their functional substitutes for body-conformable electronics, enormous effort has gone into synthesizing intrinsically soft conductors and semiconductors. In the past decades, various soft conductive and semiconducting materials have been developed and applied in body-conformable electronics, including organic materials (e.g., PEDOT:PSS, P3HT, etc.),[37,54,55,71–73] liquid-phase materials (e.g., liquid metals, liquid ions, etc.),[30,74–76] hydrogels,[77,78] nanocomposites,[79–84] etc. In this section, we highlight some skin-conformable devices utilizing these materials.

Organic conductor and semiconductors can possess innate ruggedness and bio-compatibility and hence have been researched broadly for flexible electronics.[37,54,55,71–73] For decades, their stretchability and compliance remained far from that of soft bio-tissues. However, major breakthroughs have been reported in recent years.[37] With regards to skin-conformable electronics, Zhang et al. developed stretchable and self-adhesive wearable electrodes with high conductivity (up to 545 S/cm) and low modulus (as low as 5 MPa) through solution processing of bio-compatible blends of PEDOT:PSS, waterborne polyurethane (WPU), and D-sorbitol.[71] Such PEDOT:PSS-based fully organic films have demonstrated a strong adhesion to the skin in both dry and wet conditions, as illustrated in Figures 5Ai–5Aiii.[71] P3HT is another organic material that has been studied by many researchers. For example, Guan et al. built fully stretchable rubbery transistors based on P3HT nanofilm, which was demonstrated in an elastic smart skin for pressure sensing, as shown in Figures 5Aiv–5Avi.[54] This rubbery semiconductor can maintain high electron mobility under large deformation even when stretched by 50% and can also be manufactured on a large scale.[54] Although the electronic performance is not yet on par with inorganic electronics, organic electronics has gone a long way and will continue to improve for body-conformable electronics.

Liquid phase materials including liquid metals and ionic liquid can be considered as infinitely soft and stretchable with intrinsic self-healing capabilities.[74] They have been utilized in soft electronics for various applications, including force sensors, gas sensors, thermoelectric sensors, batteries, and stretchable antennas.[74–76,86] As an example of a liquid-metal-based sensor, Figure 5B shows a skin-conformal and stretchable strain sensor, so-called the "multilayered electronic transfer tattoo (METT)".[30] The METT has an ultra-high stretchability up to 800% of strain and employs a simple layer-by-layer fabrication strategy. Figure 5Bi presents a scanning electron microscope (SEM) image of a three-layered METT. The metal-polymer conductor (MPC), composed of a gallium indium alloy and polyvinyl pyrrolidone (PVP) solution, is stacked on a poly(styrene-butadiene-styrene) (SBS) substrate. Figure 5Bii illustrates the METT sensors transferred onto a hand.[30] Figure 5C shows a

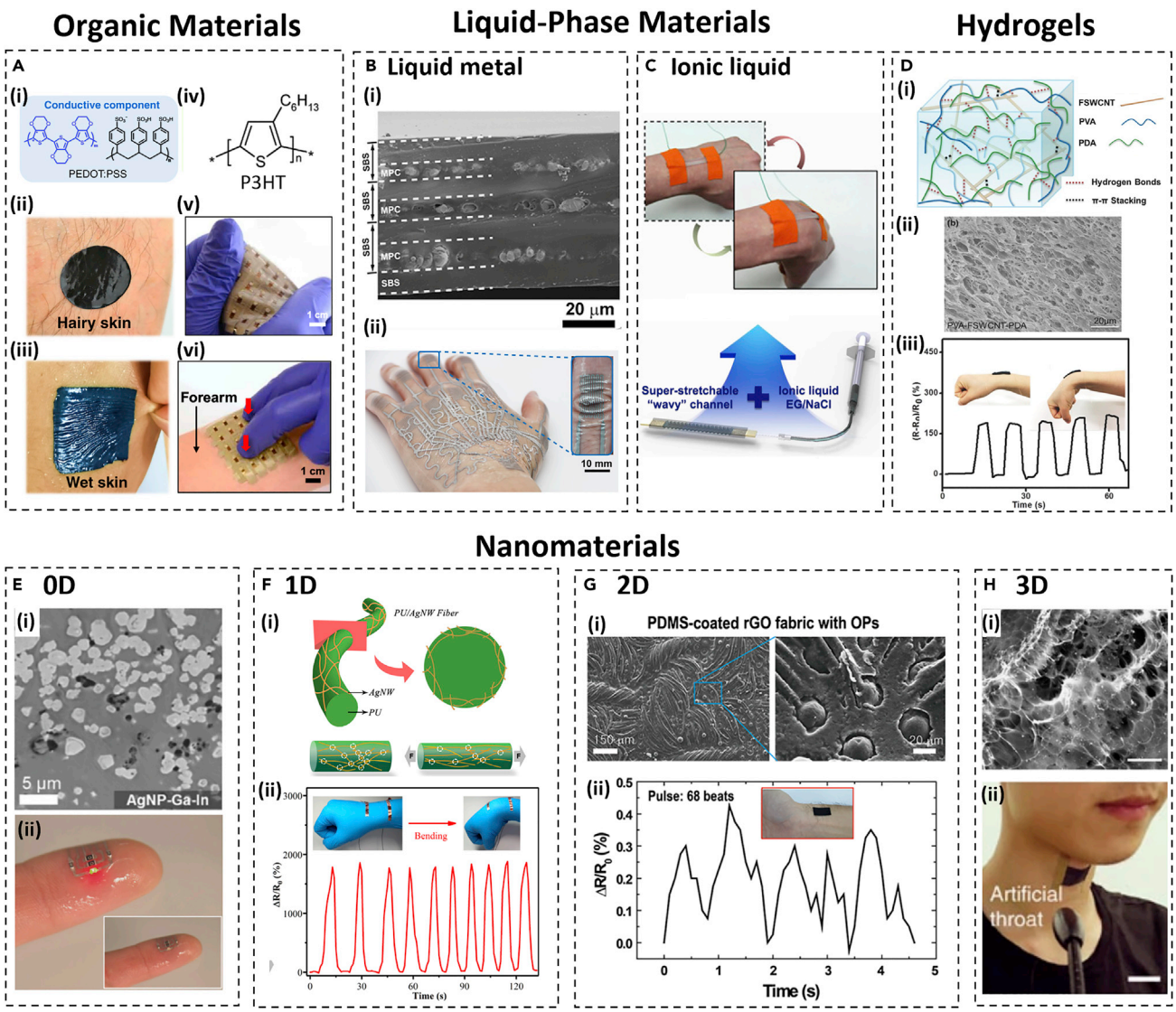


Figure 5. Intrinsically soft electronic materials

(A) Chemical structure of PEDOT:PSS and dry electrodes based on its native adhesion (i) to hairy (ii) and wet (iii) skin;[71] chemical structure of P3HT (iv)[85] and deformability of P3HT-based rubbery smart skin (v) and application on the forearm to monitor touch pressure (vi).[54]

(B) An SEM image of liquid-metal-based multilayered electronic transfer tattoo (i), and its on-skin application (ii).[30]

(C) Strain sensor based on ionic liquid of EG-NaCl with a stretchable wavy channel attached on the wrist.[76]

(D) The structure (i) and an SEM image (ii) of self-healable and -adhesive PVA-FSWCNT-PDA hydrogel, and its demonstration as a strain sensor (iii).[77]

(E) An SEM image of AgNP-Ga-In-based ink (i), and it is inkjet-printed on human finger as stretchable thin-film electrodes (ii).[80]

(F) Highly strain-sensitive and stretchable PU/AgNW fiber (i), and its application as a strain sensor on wrist (ii).[81]

(G) An SEM image of water-resistant and skin-adhesive reduced graphene oxide (rGO) fabric with octopus-like patterns (i), and its demonstration as a wearable electronics to monitor radial pulse (ii).[82]

(H) An SEM image of laser induced graphene (i), and its application as an intelligent artificial throat capable of voice sensing (ii).[83]

highly stretchable hysteresis-free strain sensor based on an ionic liquid mixture for precise joint-bending monitoring (Figure 5C, top image).[76] Ethylene glycol (EG) and NaCl were encapsulated inside a wavy, hyperelastic channel to improve the hysteresis performance of the strain sensor, as illustrated in the bottom image of Figure 5C. Despite many obvious advantages, liquid phase materials still have some challenges to overcome, such as encapsulation, electrical contact, toxicity, cost, resolution limit, and, specifically for liquid metal, surface embrittlement.[74,87]

Conductive hydrogels are composed of conductive fillers, ionic pendant groups, or salts inside crosslinked hydrophilic polymer networks. They are one of the most promising candidates for bio-integrated electronics due to their superior biocompatibility and easy-to-tune bio-adhesion. Figure 5D shows an example of a conductive hydrogel-based wearable sensor.[77] The mussel-inspired self-adhesive and conductive hybrid hydrogels were fabricated by dynamic supramolecular crosslinking among functionalized single-walled carbon nanotube (FSWCNT), polyvinyl alcohol (PVA), and polydopamine (PDA), as shown in Figure 5Di. Figure 5Dii shows an actual SEM image of the hydrogel. Furthermore, this hydrogel is self-healable by a dynamic complexing interaction between the hydroxyl group of PVA and tetrafunctional borate ions. Figure 5Diii demonstrates the application of the hydrogel as a wearable strain sensor on the wrist with self-adhesion. However, hydrogels have their own limitations, including poor environmental stability (e.g., dehydration) and limited electrochemical impedance stability.[78,88]

Another big category of intrinsically soft functional materials are composites composed of passive polymers that are doped or coated with functional micro- or nanofillers.[79,89] Depending on morphology, there are four main categories of nanomaterial fillers: 0D (e.g., nanoparticles), 1D (e.g., metal nanowires, CNTs), 2D (e.g., graphene, transition metal dichalcogenide [TMD], Mxenes), and 3D (e.g., laser-induced graphene [LIG]) materials.[79] Depending on the desired functionality, conductive, piezoelectric, and magnetic composites have been widely reported.[90,91] These functional nanocomposites typically can achieve high stretchability, chemical stability, low cost, facile solution process, and tunability of mechanical/electrical properties. However, existing challenges include relatively low performance and reproducibility. Figures 5E–5H display representative soft conductive composites based on 0D, 1D, 2D, and 3D nanomaterials, respectively.[80–83] Figure 5E shows inkjet-printed silver nanoparticles (AgNPs, 0D nanomaterial) interacting with eutectic indium gallium alloy (EGaIn) on a soft PDMS substrate, which improves the conductivity and stretchability significantly.[80] Figure 5Fi displays a strain sensor composed of PU fiber embedded with silver nanowires (AgNWs) possessing high conductivity (3.1 S/cm), elongation at break (265%), and sensitivity.[81] Figure 5Fii demonstrates the AgNW-based PU fiber as a strain sensor on the wrist. Figure 5G shows an example of a graphene-coated fabric (GCF) sensor.[82] The sensor employs octopus-like patterns on the side of the GCF that touches the skin to achieve stronger adhesion (Figure 5Gi). Figure 5Gii demonstrates radial pulse-wave measurement by the GCF attached to the wrist. Figure 5H is an example of a LIG-based wearable sensor.[83] The LIG was fabricated by scribing a polyimide film with a 450-nm laser. The 3D porous structure of the LIG is shown in Figure 5Hi. The LIG-based wearable sensor was demonstrated as an intelligent artificial throat, as shown in Figure 5Hii.[83] Moreover, a combination of 0D, 1D, 2D, and 3D dopants can yield so-called "hybrid materials," which is another avenue to improve the conductivity, stretchability, and sensitivity of wearable sensors.[84,92]

As a quick summary, Table 1 lists the Young's modulus, stretchability, and electrical conductivity of some of the representative conductors mentioned in this section. While organic conductors, hydrogels, and nanocomposites can be orders of magnitude softer and more stretchable, their electrical conductivity are still inferior to that of metals, and many nanomaterials are still costly. In short, current soft functional materials can only achieve compliance and stretchability at the expense of performance or cost. Therefore, an alternative strategy, structural engineering, has been explored as a complementary approach.

Table 1. Material property ranges pertinent to body-conformable electronics

Materials	Modulus range	Stretchability	Conductivity
Metal thin film	10–10^2 GPa	~1%	10^7–10^8 S m^{-1}
Carbon materials[91,93]	10^2–10^3 GPa	<1%	10^6–10^7 S m^{-1} (CNT)
Organic conductors[94,95]	~GPa	<6%	~10^2 S m^{-1}
Metal-based nanocomposites[96]	kPa–MPa	10%–10^3%	10^4–10^6 S m^{-1}
Hydrogel-based nanocomposites[78]	~kPa	10%–10^3%	10^{-2}–10^2 S m^{-1}
Organic-material-based nanocomposites[73]	kPa–MPa	10%–10^2%	10^5–10^6 S m^{-1}
Carbon-based nanocomposites[78,91,96]	kPa–MPa	10%–10^2%	10–10^5 S m^{-1}
Liquid-metals-based composites[97]	10^{-1}–10^2 MPa	10%–10^3%	~10^6 S m^{-1}

Structural softness

Patterning intrinsically stiff materials into specific geometries or shaping them into specific structures may significantly reduce their effective stiffness.[21,58] The earliest approach was to fabricate periodically buckled ribbons or membranes by harnessing mechanical instability.[98–100] Later, deterministically formed 3D pop-up structures enabled 3D integration between soft electronics and tissue scaffolds.[101] With encapsulation, these structures can achieve biocompatibility regardless of material composition. However, a big limitation of out-of-plane buckled structures is that they may cause mechanical irritation in long-term applications if the device is not structurally well designed.[102] As a result, buckled, pop-up, or kirigami designs are not widely used in body-conformable electronics. Instead, serpentine, fractal, and mesh designs are the preferred structures due to their negligible out-of-plane deformation and low bending stiffness.

The serpentine design, i.e., 2D meandering ribbon design, for stretchable electronics was first proposed in 2004.[103] In 2005, Li et al. pointed out that the elongation of a serpentine ribbon can be accommodated by in-plane rigid body rotation as well as minor out-of-plane buckling (Figure 6A).[104] The introduction of serpentine ribbons opened up a new paradigm for stretchable electronics. A plethora of mechanics models have been built to predict the stretchability and effective stiffness of serpentine ribbons based on their geometric parameters (e.g., width-to-radius ratio, length-to-radius ratio, and crest angle).[105–107] At first, serpentine ribbons were just used as interconnects linking rigid functional "islands." Examples include stretchable batteries,[108] integumentary cardiac monitoring devices,[38] and hydration sensor arrays (Figure 6B).[25] A major limitation of the serpentine-plus-island design is that the rigid islands still locally limit the conformability and the stretchability.[109] One remedy is to also pattern the functional materials into a filamentary serpentine network to eliminate the islands, a strategy used in epidermal electronics (Figure 6C),[5] stretchable piezoelectric sensors,[3,110] epicardial electrodes,[111] graphene e-tattoos,[17] and even glass-based stretchable photonics (Figure 6D).[112] However, serpentine designs suffer from limitations such as small areal coverage and difficulties associated with miniature devices[14] or a large number of channels.[105]

Fractal[4,26,36] and hierarchical designs[108,116] involve more advanced serpentine patterns that offer higher stretchability and areal coverage than simple serpentines. Figure 6E shows a hierarchical serpentine consisting of one large, primary serpentine constructed from many smaller, secondary serpentines.[108] Its stretchability can reach 350% due to the multistage unraveling of the primary and secondary serpentines, as shown in the figure. Moreover, compared with basic serpentines, fractal serpentines can significantly increase areal coverage, which is useful for minimizing the contact impedance between metallic electrodes and bio-tissues, as shown in Figure 6F.[2,4,26] However, fractal and hierarchical serpentines often have compromised

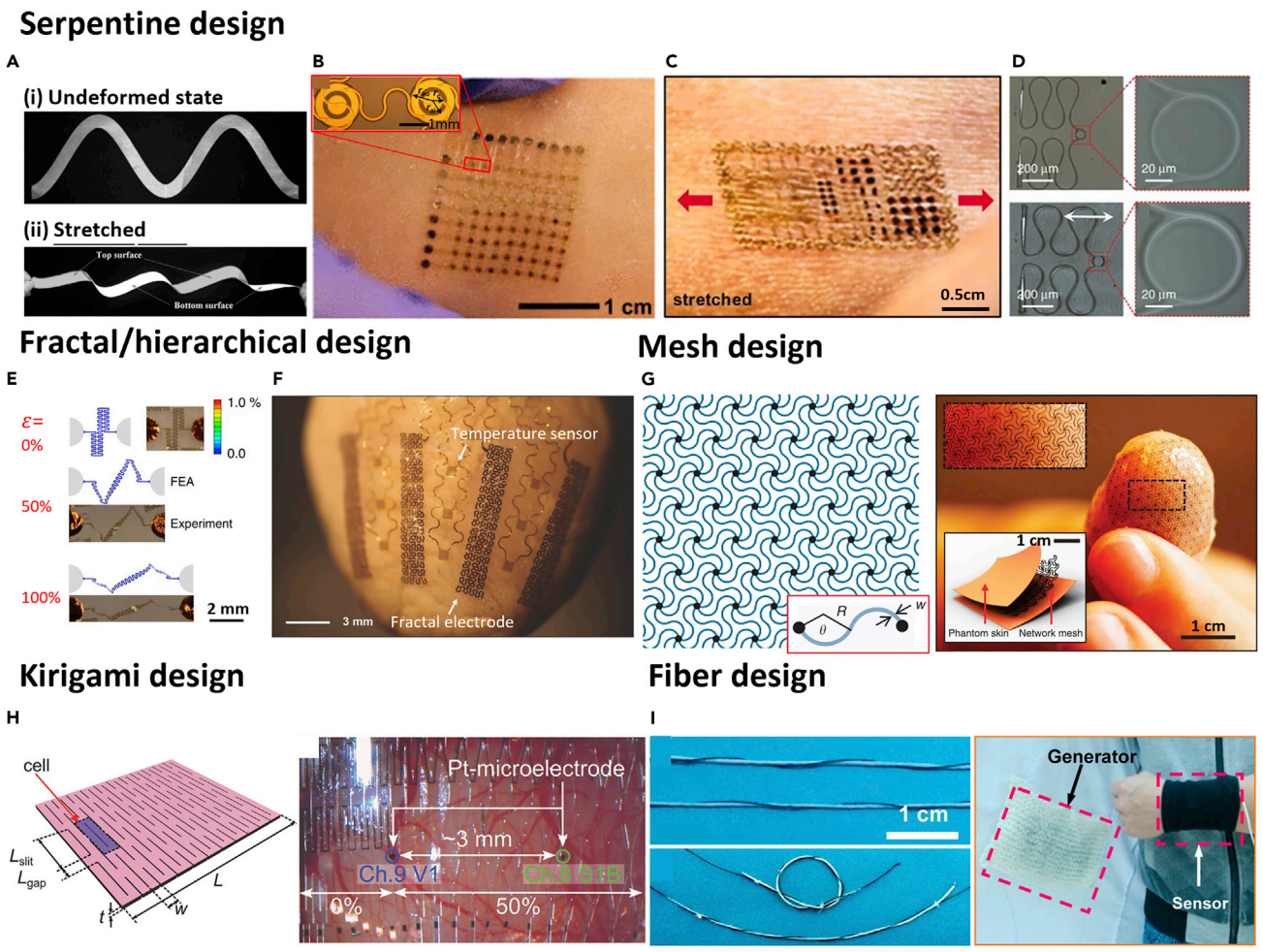


Figure 6. Examples of soft structures

(A) A paper-cut serpentine ribbon (i), and the ribbon buckled out-of-plane upon stretching (ii).[104]

(B) A stretchable hydration sensor array on skin with serpentine-plus-island design.[25]

(C) A multifunctional epidermal electronic platform with both filamentary serpentine and serpentine-plus-island design.[5]

(D) Micrographs of a glass-based stretchable photonic resonator in undeformed state (top panels) and at 36% nominal tensile strain (bottom panels).[112]

(E) Multistage unraveling of a hierarchical serpentine with fractal design under uniaxial stretching.[108]

(F) Fractal electrodes and temperature sensors for epicardial electrotherapy.[26]

(G) A serpentine mesh conformed to a fingertip.[113]

(H) Geometric parameters of a kirigami design (left) and stretchable kirigami electrodes laminated on a mouse brain for visual stimulation (right).[114]

(I) A fiber-based generator woven into a lab coat to power a wireless temperature-monitoring wristband.[115]

reversibility after large deformation and hence are more suitable for applications involving one-time stretching (e.g., fitting on a curved surface and staying in that shape).[108] Correspondingly, it is also challenging to handle fractal structures during the transfer printing process.

The mesh design involve patterning a sheet of a functional material or a device into a meshed network, often with serpentine-shaped building blocks (Figure 6G).[113] The effective stiffness of the mesh structure can be orders of magnitude lower than that of the planar sheet. For example, a filamentary serpentine mesh of polyimide offers decent stretchability (up to 57%) and a low modulus (<5 MPa) at small strains.[113] The mesh design has been used in both skin-conformable and -mimicking electronics (Figure 6G)[113] as well as in epicardial sensors with organic electrochemical transistors

Table 2. Summary of typical stretchability, advantages, and disadvantages of various soft structures

Structures	Typical stretchability	Advantages	Disadvantages
Serpentine[17,105,108]	40%–170%	planar structure; tunable stretchability; tunable effective stiffness	limited areal coverage; space taking
Hierachical or fractal designs[108,116]	70%–350%	enhanced stretchability; enhanced areal coverage	easy to entangle; hard to fully recover from
Mesh[113,117]	15%–57%	tunable stress-strain relation; low resistance due to redundancy	relatively low stretchability; risk of fracture at nodes
Kirigami[114,121]	140%–200%	high area coverage; easy fabrication	risk of fracture at cut tips; risk of damaging tissues
Buckled or pop-up structure[98]	10%–50%	medium stability; requires prestretch to fabricate	out-of-plane structure; relatively low stretchability
Fiber	~1%	bendable in all directions; easy to incorporate into fabrics	poor device performance; not stretchable; lack of fiber-manufacturing facilities

(OECTs).[117] Generally speaking, electrodes with mesh designs are not as stretchable and compliant as fractal electrodes but have more reversible deformation and lower resistance. For example, Li et al. demonstrated that a so-called "watchchain" structure provided 27% lower resistance than an equivalent serpentine due to the redundancy in conductive pathways.[118] The mesh design can also be specifically engineered to match the non-linear stress-strain behavior of human skin (Figure 6G).[113]

The kirigami design is an emerging structure used in body-conformable electronics. By adding periodic cuts in a sheet, as shown in Figure 6H, the kirigami design can be stretched up to 140% with minor mechanical force.[114] Kirigami has been increasingly utilized in stretchable electronics because it can provide the largest areal coverage among all stretchable designs.[119,120] The kirigami design has been used in integumentary electrodes on the heart or on the muscle.[114,121] A kirigami piezoelectric harvester has also been developed for energy harvesting on the human body.[122] However, kirigami has not been widely applied in implanted electronics due to the risk of fracture at the tips of the cuts and the risk of damaging the tissue from any sharp corners.

In addition to patterned thin films, nanotubes or nanofibers with superior bendability in any direction can act as biosensors individually[123] or as a nanomesh (Figure 3G).[39] Coaxial, twisted, or interlaced microfibers with diameters ranging from 10 to 100 μm can be assembled or woven into stretchable meshes.[123] For example, Zhong et al. twisted CNT fibers and polytetrafluoroethylene (PTFE) fibers together to assemble a fiber-based generator and wove it into a lab coat to power a wireless temperature-monitoring wristband (Figure 6I).[115] Lee et al. developed an ultrasensitive capacitive pressure sensor by interlacing two PDMS-coated conductive fibers.[124] However, the difficulty in fabricating the unique fiber structure is a tradeoff for its excellent mechanical properties.[125]

Innovative structural designs have advanced the capabilities of body-conformable electronics by reducing the effective modulus and increasing the stretchability of a wide variety of conventional electronic materials. However, there is an intrinsic trade-off between the mechanical performance and the size of the structure. Typical stretchability, advantages, and disadvantages of these structures are summarized in Table 2.

STRATEGIES FOR ADHESION ENHANCEMENT AT THE BIO-ELECTRONICS INTERFACE

Robust interfacial adhesion is crucial for stable and long-term conformability between soft electronics and dynamic bio-tissues. On the one hand, the thickness

and stiffness of many devices cannot be further lowered without compromising functionality. For these devices, native adhesion is far from enough for a secure bio-attachment, thus necessitating adhesion engineering to enhance their conformability. On the other hand, although some soft electronics can fully conform to bio-tissues by increasing device compliance, large and/or repetitive tissue deformation can degrade the attachment over time.[65] To address these issues, there is an urgent need for adhesion-promoting strategies for the bio-electronics interface.

However, many conventional adhesives such as cyanoacrylates are not biocompatible (both chemically and mechanically). Even though the maximum adhesive strength of acrylic adhesive on the skin can reach 30 kPa (see Figure 2Dii),[126] these adhesives not only cause skin irritation but also have limited reusability.[41] To overcome these limitations, physically and chemically enhanced biocompatible adhesives for both dry and wet tissues are reviewed below.

Dry adhesion

When soft devices are attached to dry bio-tissues such as the skin, physically enhanced adhesives (also known as dry adhesives) are popular candidates owing to their reversibility and reusability. Possible physical interactions include van der Waals and electrostatic forces, suction, and friction.[127] Ultrathin epidermal electronics and e-tattoos can well conform to the skin purely through van der Waals forces, but thicker ones require stronger adhesion.[5,17,39] The most widely studied physically enhanced adhesives are structured surfaces with arrays of micro-pillars[60] or micro-craters,[128] as shown in Figures 7A and 7B, respectively.

Bartlett et al.[129,130] has demonstrated that the adhesive force of micro-pillars, originating from van der Waals interactions, can be scaled as

$$F_{ad} \sim \sqrt{\frac{A}{C}}, \qquad \text{(Equation 2)}$$

where A is the actual contact area and C is the system compliance in the loading direction. Benefiting from high-aspect-ratio hairy structures, micro-pillars can easily deform to accommodate rough bio-surfaces, as shown in Figure 7A (right panel).[60] As a result, the contact area A is enlarged. Moreover, the Ashby plot of normal adhesive strength versus Young's modulus in Figure 7C (note: Figure 7C is not limited to just bio-surface adhesion) exhibits the reciprocal relationship between the adhesive strength and the compliance of the materials constituting the micro-pillars (purple zones).[127] The adhesive strength of the micro-pillar arrays has been further optimized through the design of various tip shapes.[126,131] For example, the adhesive strength of micro-pillar arrays with mushroom-shaped tips on skins can reach 18 kPa because of reduced contact stress concentrations, compared with 4 kPa of plain pillars.[132]

However, micro-pillar-based dry adhesives have several limitations. First, the high aspect ratio of micro-pillars makes them prone to buckling, entanglements, and fracture, which degrades their adhesive performance. Second, although the "contact-splitting" theory suggests that enhanced adhesion can be achieved by splitting up the contact region into finer sub-contact regions,[133,134] manufacturing difficulties and associated costs dramatically increase as the pillar size scales down to nanometers, thus enacting a practical limit to the achievable adhesion. Third, the van der Waals interaction does not operate in wet environments, thus precluding the application of pillared adhesives to wet surfaces.[135]

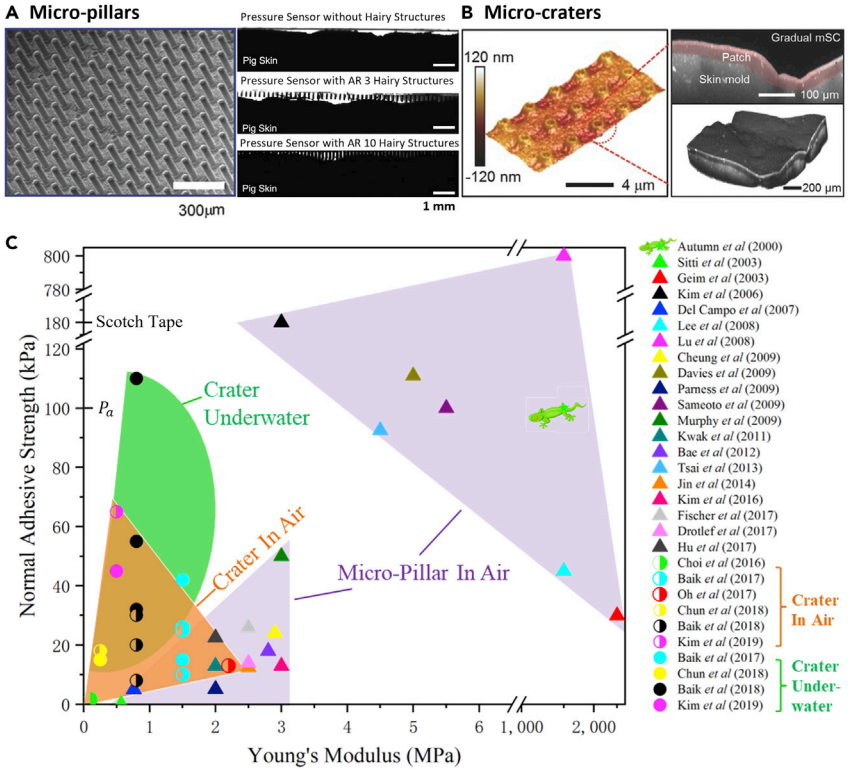


Figure 7. Examples and summary of physically enhanced adhesives, also known as dry adhesives

(A) Left: an SEM image of an array of micro-pillars with a 30-μm radius and an aspect ratio (AR) of 10. Right: the cross-sectional views of pressure sensors with micro-pillars of different ARs (0/3/10) on pig skin (right).[60]

(B) A 3D atomic force microscopy (AFM) image of a micro-crater array (left) and confocal microscope images (cross-sectional and 3D views) of patch/skin interface.[128]

(C) An Ashby plot of normal adhesive strength versus material Young's modulus for both pillar- and crater-based dry adhesives.[127] Compared with pillars, craters are able to achieve higher adhesion out of softer materials.

To overcome these limitations, another category of dry adhesives, micro-crater arrays, has been explored.[127] Figure 7B shows a confocal microscope image of a skin patch with an array of micro-craters on the surface.[128] In ambient environments, the suction force generated by expelling the air out of the crater upon deformation dominates over the van der Waals interaction. Therefore, the adhesive strength can be obtained as

$$\sigma_c = \left(1 - \frac{V_1}{V_2}\right) p_0 \frac{A_2}{A_0}, \qquad \text{(Equation 3)}$$

where A_0 and p_0 are the projected area and the inner pressure of the crater at the initial state, respectively, V_1 is the volume of crater under preload, and V_2 and A_2 are the volume and the projected area after the preload is fully released, respectively.[136,137] The "crater-in-air" group (orange zone) in Figure 7C indicates that cratered surfaces are able to achieve higher adhesion with softer materials than are pillared surfaces. This finding is especially important considering that device compliance is a key parameter that controls conformability, as noted in conformability model and examples. The maximum adhesive strength between cratered surfaces and the dry skin can reach 20 kPa[138] (approximately one-tenth of the adhesive strength of the Scotch tape). Cratered surface adhesives were reported to be able to

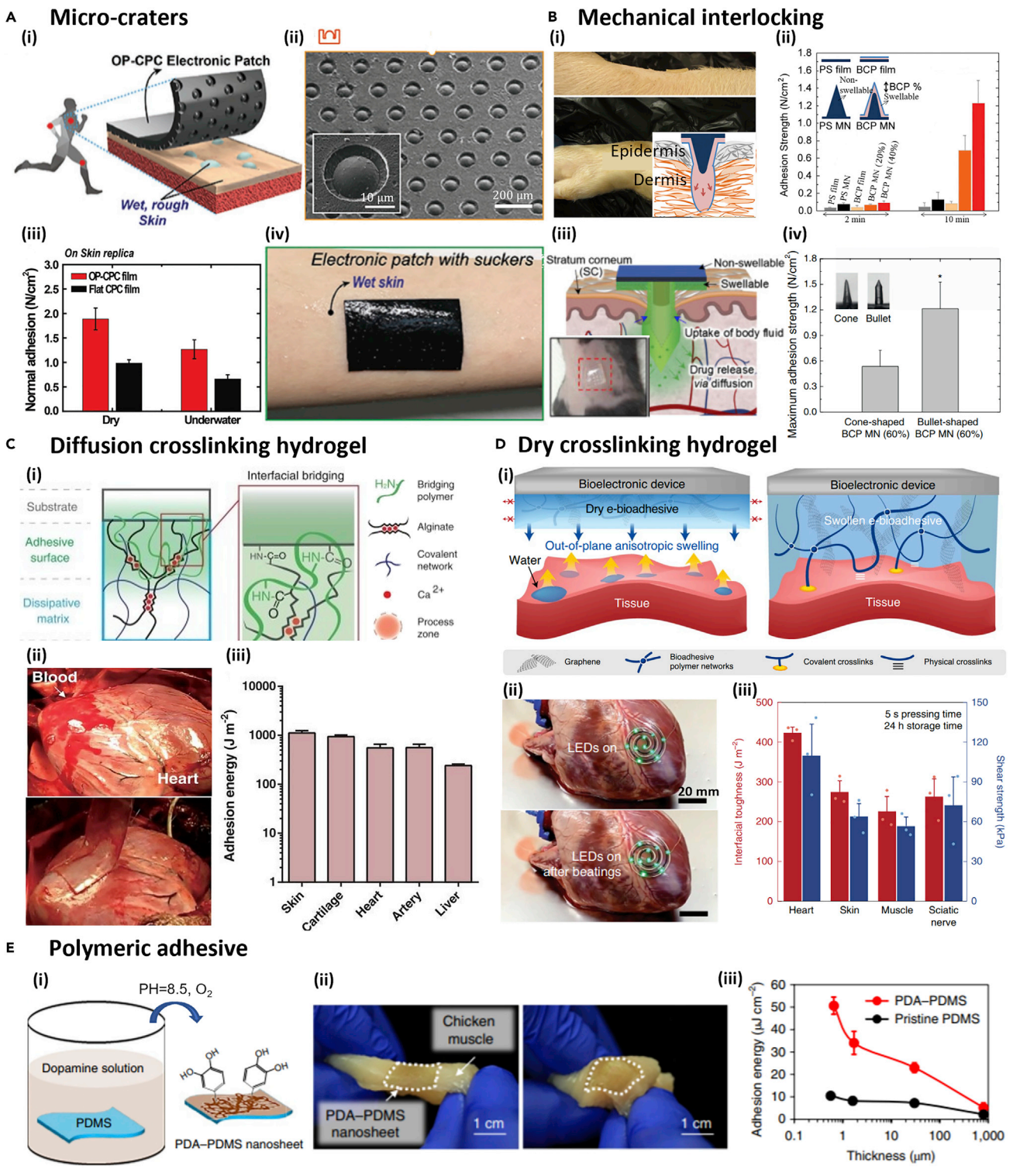


Figure 8. Strategies to enhance bio-electronics adhesion in wet environment

(A) A schematic illustration (i) and an SEM image of an electronic patch with micro-craters (ii), the normal adhesion for octopus-like carbon-based conductive polymer composite (OP-CPC) substrates in dry and underwater environments (iii), and a photo of the OP-CPC on wet skin (iv).[138]

(B) A flexible block copolymer microneedle (BCP MN) array on a shaved pig wrist and the mechanical interlocking formed by the MN with a non-swellable core and a swellable coating (inset) (i), normal adhesive strengths for PS and BCP films, PS MNs, and BCP MN adhesives with 20% and 40%

Figure 8. *Continued*
swellable tip-height fractions after insertion into skin for 2 and 10 min (ii),[140] a schematic of a bullet-shaped biphasic MN inserted into the skin (iii), and normal adhesive strength of cone-shaped BCP MNs versus bullet-shaped BCP MNs (iv).[141]
(C) Tough hydrogel adhesives composed of a dissipative matrix and an adhesive surface based on the diffusion-crosslinking mechanism (i), application of the tough adhesive on porcine heart with blood exposure (ii), and interfacial toughness with various tissue surfaces (iii).[61]
(D) Design and mechanism of e-bio-adhesive based on the dry-crosslinking mechanism (i), LEDs with the e-bio-adhesive attached to a porcine heart before/after heart beatings (ii), and interfacial toughness and shear strength between polyimide and various tissues attached by e-bio-adhesive (iii).[62]
(E) Schematics of polydopamine (PDA) modification of polydimethylsiloxane (PDMS) nanosheets (i), images of a PDA–PDMS nanosheet on chicken muscle while the tissue was stretched (left) and contracted (right) (ii), and the relationship between thickness and adhesion energy to chicken muscle for pristine and PDA-modified PDMS (iii).[142]

reach 110-kPa normal adhesive strength on Si wafer underwater,[139] but more validations on bio-surfaces are needed. Despite promising preliminary work, the mechanics of micro-craters require deeper investigation to fully unveil their working principles and enable future innovations.[136,137]

Wet adhesion

Wet environments are very common for bio-tissues due to the presence of body fluids, such as sweat, blood, and interstitial fluid. Such environments pose unique challenges as well as opportunities for body-conformable electronics. Some physical interactions like the van der Waals and the electrostatic forces are dramatically weakened by the existence of liquids. Conversely, body fluids offer unique opportunities for enhancing adhesion because fluids can facilitate swelling, chemical reactions, and the diffusion of polymer chains. In the following section, we showcase physically and chemically enhanced adhesives that have proven effective for bio-adhesion under wet conditions.

Octopus-inspired micro-craters with protuberances (Figures 8Ai and 8Aii) have been reported to enhance attachments to skin under both dry and wet conditions.[138] Figure 8Aiii plots the normal adhesive strength of a flat carbon-based conductive polymer composite (CPC) film and an octopus-like CPC (OP-CPC) film with micro-craters under both dry and underwater environments. From the figure, it is obvious that the OP-CPC films provide stronger adhesion than the flat CPCs under both conditions, achieving up to 12 kPa underwater. Its attachment on skin as an electrode for electrophysiological sensing is demonstrated in Figure 8Aiv.

While micro-crater-based adhesives are non-invasive, there are also minimally invasive physical methods for enhancing bio-attachment such as mechanical interlocking. Figure 8Bi shows a biphasic microneedle (MN) structure consisting of a non-swellable core composed of polystyrene (PS) homopolymer (blue) and a swellable, water-responsive coating composed of PS-block-poly(acrylic acid) (PS-b-PAA) block copolymer (BCP) (pink).[140] After penetrating the skin, the tip of the BCP comes into contact with the aqueous dermis and swells, while the part in contact with the water-free epidermis remains unswollen. Therefore, a mechanical interlock is formed, as illustrated in Figure 8Bi. It generates strong, effective interfacial adhesion in both the normal and tangential directions, as summarized in Figure 8Bii. The normal adhesive strength provided by the MNs on skin surfaces is up to 12 kPa (as shown in Figure 8Bii) and can reach up to 45 kPa on mucous-wet intestine surfaces. Furthermore, Figure 8Biii shows that an additional enhancement of on-skin adhesion can be achieved by tuning the shape of the MNs from a cone to a bullet shape, which increases the normal adhesive strength to 16 kPa, as shown in Figure 8Biv.[141]

Since physical interactions are reaching their limits, chemical bonding has been widely explored to elevate bio-electronics interfacial adhesion to another scale.

Given their bio-compatibility and multifunctionality, hydrogels have become popular adhesives between dynamic tissues and electronics.[143–145] A diffusion-crosslinking tissue-hydrogel interface is shown in Figure 8C.[61] The slug-inspired tough adhesives (TAs) consist of an adhesive surface touching the tissue and a dissipative matrix on the back. The adhesive surface contains a positively charged interpenetrating polymer that forms covalent bonds with the tissue surface, as shown in Figures 8Ci and 8Cii. The tough dissipative matrix can help dissipate energy through hysteresis when the interface is stressed. As a result, ultra-strong adhesion, e.g., up to 1,000 J/m^2, can be formed on various bio-tissues, as shown in Figure 8Ciii. Compared with hydrogel adhesives based on the diffusion-crosslinking mechanism, which usually requires 5–30 min to form stable bonding, those capable of dry crosslinking (Figure 8D) can provide much quicker (i.e., a few seconds) chemical bonding between the swellable adherend and the underlying tissue.[62,146] Such an interface provides exceptional interfacial toughness (maximum around 420 J/m^2) and shear strength (maximum around 110 kPa), as shown in Figure 8Diii. Additionally, it can be easily removed without tissue damage via triggering solutions, which cleave the hydrogen bonds and the covalent disulfide bonds formed at the interface. The mechanism of such triggerable detachment was reported in detail by Chen et al.[147] and is called instant tough bio-adhesive with triggerable benign detachment.

Biocompatible polymeric coatings can also enhance bio-electronic adhesion. For example, Figure 8E shows a strategy of enhanced bio-adhesion enabled by a polydiacetylene (PDA) coating on PDMS film. The coating procedure is illustrated by Figure 8Ei: a PDA as thin as 50 nm can be coated on PDMS film by simply immersing the samples in a dopamine solution at a pH of 8.5. Thereafter, Figure 8Eii shows strong bonding between the PDA-coated PDMS and the chicken muscle even under tension/compression. The adhesion energy between PDA-coated PDMS and bio-tissue (up to 0.5 J/m^2) is highly improved compared with that between pristine PDMS and bio-tissue (up to 0.1 J/m^2) (Figure 8Eiii).[142] A more recent work shows that PDA-coated Ecoflex also exhibits enhanced adhesion at bio-electronic interfaces, even after extended period of time (e.g., 1 month).[148]

The adhesion-enhancement strategies reviewed above are powerful tools to improve the attachment of electronics on bio-surfaces. However, as the structural and material properties of the devices grow in complexity, innovative bio-integration strategies must be leveraged to further facilitate body conformability.

EMERGING BIO-INTEGRATION STRATEGIES

As bio-electronics are becoming thinner, softer, and stickier, their manipulation becomes increasingly difficult and requires special techniques. Therefore, new methods for integrating electronics to bio-tissues (i.e., bio-integration strategies) have been developed to overcome the challenges in handling and deploying soft electronic devices. Herein, we showcase how emerging wearable and implantable bio-integration strategies can promote body conformability.

Integration of wearable devices

In recent decades, various transfer printing methods have been developed to non-invasively integrate substrate-free ultrathin sensors on human skin. The first transfer printing method, stamp transfer printing, was borrowed from micro-fabrication.[149] With an elastomeric stamp as a temporary support, devices in filamentary serpentine mesh designs are retrieved from a donor substrate, such as a silicon wafer, where they had been micro-fabricated on. Then, the devices are transferred to a skin

surface presprayed with an adhesive, as shown in Figures 9Ai–9Aiii.[150] This method is easy to implement but is not compatible with surfaces of large Gaussian curvatures. Hence, water-assisted transfer printing was proposed, as shown in Figures 9Ai and 9Aiv–9Avi.[150] It utilizes a thin PVA film instead of the elastomeric stamp as the temporary support. Because the PVA can be dissolved by simply smearing water, prespraying an adhesive on the skin is no longer required. Without the thick elastomeric stamp, the electrodes can be transferred to surfaces with moderate curvatures. However, the transfer is path-dependent and thus is usually not reproducible and also requires time to dry.[17,69] As a result, these two methods are more suitable for transferring small-scale (e.g., cm-scale) devices. When the device size is large (e.g., beyond 10 cm), the transfer yield degrades dramatically due to filament distortion, entanglement, and even fracture. To address these limitations, a Cartan transfer printing method was developed for large-area electrodes to perform multichannel ECG or EMG.[4] This method was inspired by the mathematics concept of the Cartan connection; in transfer printing, this means that the non-slippery, point-by-point contact helps minimize the transfer-induced strain. Therefore, the thin donor substrate (e.g., a piece of fabric) keeps rolling on the target surface with the goal of forming only small-area contact at any given time, as shown in Figure 9Bi.[4] Figure 9Bii shows a 16-channel, substrate-free, filamentary-serpentine-based EMG sensor Cartan-transfer-printed on a human neck with the original pattern well preserved. However, Cartan transfer printing is more time consuming than one-time, full-area lamination, especially considering the large area. For unpatterned ultrathin blanket sheets, pipette transfer is possible, as shown in Figure 9C.[151] A 230-nm-thick PEDOT:PSS-sandwiched AgNWs film is first placed in water. A pipette sucks up the water containing the nanomembrane and then delivers the water and film altogether to the skin. Due to surface tension, the nanomembrane expands and conforms to the skin after water evaporates.[152] However, pipette transfer only works for ultrathin, uniform sheets without any patterns, as the pattern can easily become distorted or entangled during the pipette suction or delivery.[151]

The aforementioned transfer methods aim to integrate substrate-free ultrathin devices on bio-tissue, which are the simplest solutions for ensuring body conformability, as explained in conformability model and examples. When thicker devices are involved, one good approach is to fabricate the devices on a substrate that is preshaped to have matching curvatures with the target bio-surface. For example, multimodal sensors can be integrated on a glove, which is already in a hand shape, as shown in Figure 9D,[7] and a smart contact lens for non-invasive but continuous glucose monitoring can be fabricated on a dome-shaped substrate, as shown in Figure 9E.[8] Preshaped electronics can naturally conform to the target tissue but may require customization due to individual differences in tissue geometry. Since these electronics require substrates, it is worth noting that the bio-integration process must not impose excessive mechanical loading or constraints to the tissue nor interfere with the physiological functionality of the organ.

Integration of implantable devices

Tissue and organ geometries inside the human body are highly diverse. This section categorizes bio-integration strategies based on different tissue topologies and does not include the surgical procedures. For applications on surfaces with near-zero Gaussian curvatures, direct lamination or insertion is feasible, such as directly wrapping e-dura over the spinal cord (Figure 3D),[12,49] laminating sensors on the heart surface,[117] or inserting optogenetics patches under the skull (Figure 9F).[13] To account for more complex geometries, a few unique integration methods have been developed. For example, since smart stents must be installed against the inner arterial

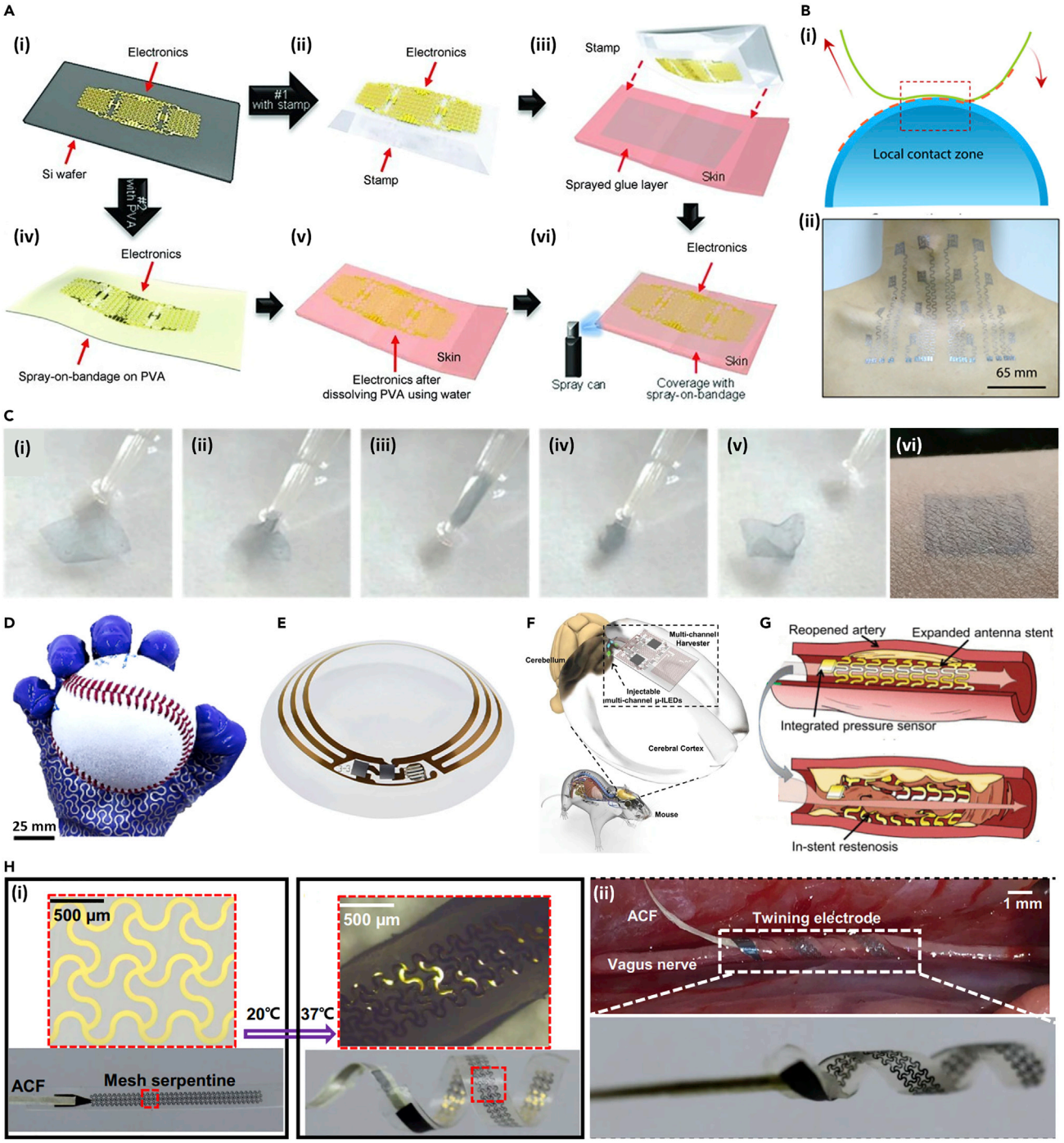


Figure 9. Bio-integration methods for wearable and implantable devices

(A) The process of stamp transfer printing (i-iii and vi) and water-assisted transfer printing (i and iv-vi) on skin.[150]

(B) The concept of Cartan transfer printing (i) and large-area, neck-conformable electrode array Cartan-transfer-printed with high fidelity (ii).[4]

(C) The process of pipette transfer printing (i-v) and an ultrathin film transferred to human skin (vi).[151]

(D) Tactile and motion sensors directly integrated on a glove.[7]

(E) Glucose sensors fabricated on a contact lens.[8]

(F) An optogenetic device on a mouse brain by direct lamination.[13]

(G) Balloon-catheter-assisted deployment of a smart arterial stent.[28]

(H) A serpentine mesh on a shape memory substrate, which is flat at 20°C but spiral at 37°C (i), and the electrode self-climbed and twined around the nerve after implantation (ii).[29]

wall, a balloon-assisted transfer method was developed for bio-surfaces with negative curvature, as shown in Figure 9G.[28] First, the stent is shrunk and wrapped around a catheter with a balloon. After reaching the target location within the artery, the balloon is inflated and expands the smart stent to push against the arterial wall from the inside. Finally, the catheter is deflated and removed, leaving the plastically expanded stent inside the artery. Similarly, an instrumented multifunctional balloon catheter can make contact with the endocardial wall through inflation for radio frequency (RF) ablation treatment.[153] For nerve integration, devices need to wrap around slender and delicate nerve tissue without causing damage. An innovative temperature-actuated helical ribbon of electrodes in serpentine mesh was devised using a shape-memory substrate. It is flat under room temperature (Figure 9Hi) but is programmed to twine and self-climb on the nerves like a vine at body temperatures (i.e., 37°C), as evidenced in Figure 9Hii.[29]

Unfortunately, there is no universal bio-integration strategy given the excessive variables involved. Ideal bio-integration methods must minimize the deformation in both the tissues and the electronics while maximizing conformability and stability. Therefore, the bio-integration method is also an important and diverse area of research for body-conformable electronics.

OUTLOOK

Despite extensive research, there are still many outstanding challenges for body-conformable electronics, such as the poor conformability of flexible but non-stretchable devices, the incorporation of microcontrollers and wireless communication without adding stiffness, the customization of bio-electronics for personal use, and skin-contact-impeding factors such as hair and sweat. Therefore, this section discusses emerging potential or partial solutions to these challenging issues and concludes with a few personal expectations for the future directions of body-conformable electronics.

Conformability of non-stretchable thin-film electronics

As noted before, a major limitation of structurally optimized stretchable electronics is their low areal filling ratio of the functional components. This is not a significant problem for many bio-integrated electronics; however, for optoelectronics[14,154] and energy systems,[155] the density of functional components directly impacts their key figure of merits. To remain high density, stretchability has to be compromised in many cases. It is well known that non-stretchable electronics are only able to wrap around cylindrical surfaces but cannot fully conform to surfaces with non-zero Gaussian curvatures. For example, when a stiff thin film tries to conform to a spherical substrate, radial buckle delamination occurs at the edge of the film due to hoop compression.[156] Buckle delaminations are undesirable for high-density devices because they induce excessive strains and distortions and are unstable and uncontrollable. To achieve full conformability in such cases, a kirigami-inspired design was proposed, as illustrated by Figure 10A.[14] A 1.4-μm-thick and 9.3-mm-diameter artificial retina could house 1,935 2D-material-based photodetectors while fully conforming to a hemispherical surface without forming any buckles through a truncated icosahedron design inspired by soccer balls.[14] This design was also modeled by the finite element method (FEM) and proved effective in eliminating buckle elimination compared with intact circular sheets.[14] It differs from the conventional kirigami design shown in Figure 6H because the cuts must be made strategically to achieve perfect conformation. A generic computational method was developed to obtain the optimal cuts in a planar film to perfectly conform to arbitrary 3D-curved surfaces



Figure 10. Possible solutions to remaining challenges in body-conformable electronics

(A) A cut-enabled non-stretchable but conformable ultrathin image sensor array as an artificial retina conformed to a dome mimicking the eyeball.[14]

(B) A multilayer, modular, reusable, and reconfigurable wireless e-tattoo platform that is still stretchable and robust after incorporating rigid ICs.[24]

(C) An octopus-like patch on a hairy skin.[139]

(D) The process of direct drawing with stencils (i–iv), and the epidermal electronics system fabricated by direct drawing (v).[18]

(E) An electrode printed on a finger.[158]

(F) Electronics directly printed on the back of the hand by a 3D printer.[159]

(G) On-body printing through a portable inkjet printer.[160]

(H) A highly transparent and breathable epidermal electrode composed of AgNWs and reinforcement polymer nanofibers.[161]

(I) Temperature sensors sandwiched by semipermeable film after wearing for 24 h.[162]

(J) A gas-permeable porous electrode.[163]

with maximum coverage.[157] However, this geometric model assumed a negligible thickness of the film and therefore does not account for mechanics and manufacturability. Mechanics models that consider the strain and adhesion energies are not yet available to fully guide the planar design of non-stretchable, thin-film electronics intended to conform to 3D bio-surfaces with non-zero Gaussian curvatures.

Modular and reconfigurable electronics

Enabling the wireless operation of body-conformable electronics is challenging because the analog front end, signal processing, and wireless communication circuitries typically rely on silicon-based integrated circuits (ICs), which are intrinsically rigid and are designed to be soldered on conventional rigid printed circuit boards (PCBs). While flexible printed circuits (FPCs) are becoming more available commercially, their thinness and compliance are still insufficient for body-conformable electronics. Therefore, the 3D construction of multilayer, integrated, stretchable electronics was developed through laser ablation and controlled soldering processes to create vertical interconnects between transfer-printed layers.[164] A similar but lower-cost solution emerged as the multilayer modular wireless e-tattoo, as displayed in Figure 10B.[24] The e-tattoo consists of a reusable near-field communication (NFC) layer, a replaceable functional layer, and an optional replaceable electrode layer. Within each layer, the filamentary serpentine design of the 18-μm-thick copper interconnects laminated to a 7-MPa-modulus Tegaderm medical dressing enables high stretchability of the e-tattoo. In the thickness direction, the soft Tegaderm substrate of each layer serves as a soft interlayer, which offers the split-of-neutral-axis effect.[67] This effect decouples the bending of each stiff layer and has proven effective for reducing bending stiffness and bending-induced strains.[67,68] The modular design also enables reconfigurability of the e-tattoo because the different layers can be disassembled, swapped, and reassembled, like the stacking up and swapping of LEGO pieces. This reconfiguration enables both the rapid customization of functionalities and the hygienic reuse of the e-tattoo on different subjects after replacing the bottom electrode layer. It is worth pointing out that other reconfigurable e-tattoos exist, for example, enabled by liquid metal and self-healable polymers.[165,166] However, thinner and softer wireless e-tattoos require further development, such as the utilization of bare dies instead of packaged chips.[167]

Electronics on hairy skin

The human skin is covered by a wide variety of hairs, including thick hairs on the scalp and fine hairs elsewhere. Unfortunately, these hairs impede the conformal contact with wearable devices and will cause pain when adhesives are pulled off upon device removal. Inapplicability on hairy skin is a well-known and long-standing limitation of epidermal electronics or e-tattoos. Emerging physically enhanced adhesives and on-body drawn or printed electronics have shed some light. Figure 10C shows a bio-mimetic dry adhesive design.[139] This patch can conform and adhere to the skin due to the suction force of the micro-craters. Experiments have demonstrated that micro-craters produce three times stronger normal adhesion than their flat counterpart on hairy pig skin.[139] Gentle peeling of the patch easily breaks the suction in the micro-craters, which allows delicate removal without hurting the hair. However, such cratered dry adhesive cannot not work on the highly hairy scalp. EEG sensing on the human head is notoriously tedious and expensive, partially due to the one-by-one gel electrode application for each EEG channel. Dry EEG electrodes have been engineered by 3D molding a conductive polymer into finger-like structures to penetrate past the hairs and contact the scalp. These electrodes usually require a bulky headset with supporting frames or bands to enforce the contact between the 3D dry electrodes and the scalp.

The emergence of direct drawing or printing of bio-compatible and body-temperature-formable electrodes on the skin is a promising potential solution for hairy skin. However, the technology is still in its infancy. With a stencil and modified ballpoint pen, Ershad et al.[18] directly drew on the human skin with conductive Ag-PEDOT:PSS composites, semiconducting P3HT-NF, and dielectric ion gels, as shown in Figures 10Di–10Div. A more complicated electronics system can be drawn on the skin, as shown in Figure 10Dv. It has been found that the drawn-on-skin system is stable, reliable, and strongly adherent to hairy human skin.[18] To automate the process for improved repeatability and customization, direct printing with 3D printers or inkjet printers has been explored. With an inkjet printer, more complicated patterns can be printed at various curved surfaces on the human body, as shown in Figures 10E–10G.[158–160] So far, researchers have only shown the preliminary possibility of direct printing on human skin. The printing accuracy on soft curvilinear and mobile bio-surfaces and the ink variation require more exploration. The versatility and tunability of direct printing show good promise in body-conformable electronics, especially for hairy skin, for the following two reasons. First, the printer head can potentially be inserted close to the root of the hairs to print the ink directly on the scalp skin. The ink can wet the skin surface with high conformability. Second, since the ink dries and cures on the skin, hairs would have a smaller effect on the ink adhesion to the skin. Ultimately, the tunable ink, easily customizable design, and on-tissue digital printing of electronics could enable unprecedented personalization for body-conformable electronics.

Breathable electronics

In addition to hairs, sweat is another inevitable degrader of device-skin interfacial adhesion, especially during long-term application. Intuitively, substrate-free, mesh-like e-tattoos can provide good sweat tolerance due to the uninhibited evaporation of the sweat. For example, electrodes composed of AgNWs on nanofibers (Figure 10H)[161] or gold nanomesh designs[39] have been developed to enable gas and fluid permeability. When a substrate must be used, it is desirable for it to be also fluid and gas permeable. For example, Jang et al. fabricated bio-electronics on a fabric patch with a silicone adhesive layer, allowing sweat to evaporate through the porous fabric.[168] Figure 10I demonstrates a temperature sensor attached to the forearm for 24 h without delaminating or inducing any skin irritation. The device is encapsulated by a semipermeable film, so it is permeable to sweat while also being waterproof to external liquids.[162] For better permeability, Zhou et al.[163] (Figure 10J) and Yeon et al.[169] intentionally patterned through holes on the substrate and/or the device to allow moisture to escape. Future advancements in permeable electronics should aim for thinness, strong adhesion, and ease of fabrication and manipulation. Sometimes, sweat could be useful. For example, the electrolytes in sweat are helpful in lowering the contact impedance for electrophysiological sensing.[9,170] As sweat contains abundant analytes secreted from the body,[171] it has been increasingly popular bio-fluid for non-invasive chemical bio-marker analysis.[9,172,173]

CONCLUSIONS

Although we use conformability model and examples to guide the discussion in terms of device thinness, device softness, and bio-electronics adhesion, we acknowledge that this model cannot encompass all relevant factors. A successful body-conformable electronic device requires more comprehensive strategic planning. Therefore, in Figure 11, we attempt to highlight the multifaceted nature of this problem and emphasize a holistic strategy for achieving

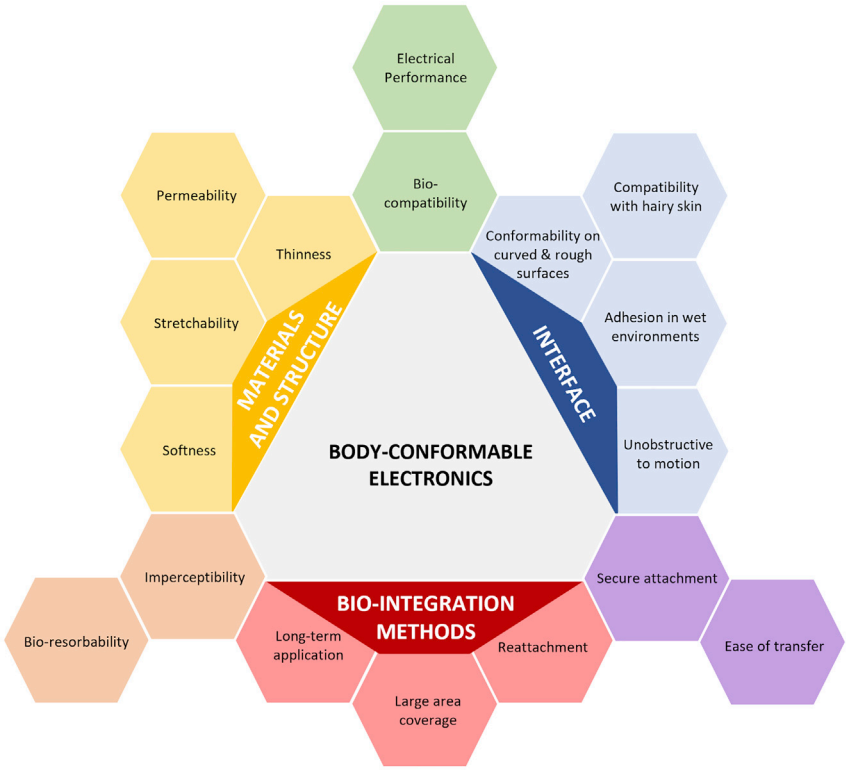


Figure 11. An illustration for the holistic approach when designing and evaluating body-conformable electronics

biologically safe, mechanically reliable, and functionally superior body-conformable electronics. We categorize the holistic strategy into three aspects: materials and structures (yellow), bio-electronics interface (blue), and bio-integration methods (red). These three aspects may have overlaps and interactions, which are also considered.

In the materials and structural design, meaningful advancements have been made to improve device thinness, stretchability, and curvature matching with the bio-surface. However, materials with combined mechanical compliance and high electronic performance warrant further research and innovation. In this review, we have focused on three aspects under this category, specifically, device thinness, intrinsically soft materials, and stretchable mechanical structures.

Next, the bio-electronics interface suffers from a wide variety of complications. Curved, rough, moving, wet, and hairy surfaces are ubiquitous in the human body and can severely influence the quality and longevity of contact. In addition, the interfacial design can significantly impact the device's biocompatibility, electrical performance, long-term survivability, and ability to be securely attached and easily removed. Strategies to enhance the interfacial adhesion under both dry and wet environments have been summarized in this review.

Finally, in addition to material/structural and interfacial designs, novel bio-integration methods can further facilitate body conformability, especially when the device is too thin or too large to handle or when the organ curvature and geometry are unique. In addition to surface-conformable electronics, there have been many

innovative methods developed for the 3D deployment of soft electronics to spatially couple with bio-tissues. Examples include the syringe-injectable, deep-brain-monitoring electrode mesh[174] and the implantation of stretchable nanoelectronics via organogenesis.[175] More discussions on 3D bio-electronics integration can be found in two recent reviews.[20,176]

The three aspects described above do not act in isolation. Rather, there are complex interactions between the materials and structure, the interface, and bio-integration methods that must be considered when optimizing body-conformable electronics. For example, both the material and the interface dictate the device performance. Specifically, gel electrodes offer low contact impedance to the skin due to interfacial electrochemical activities, whereas the graphene e-tattoo, despite a dry electrode, affords comparable contact impedance to gel electrodes due to the perfect conformability to the skin. As another example, to achieve secure tissue attachment, both robust interfacial design and interface-compatible bio-integration methods must be developed. Moreover, device removal is a big topic inverse to bio-integration. Transient and bio-resorbable electronics can eliminate the needs of additional surgical procedures for device extraction. This exciting frontier of bio-electronics heavily relies on advancements in material engineering and bio-integration.[177–179]

At last, bio-compatibility requires consideration of the device materials, the interface design, and even the bio-integration methods specifically for implantable applications. Many methods have been developed to ensure bio-compatibility for bio-electronics. First, intrinsically bio-compatible materials can be directly used. Many widely used organic materials (e.g., PEDOT:PSS, P3HT, and Phenyl-C61-butyric acid methyl ester),[180] some liquid-phase materials (e.g., EG-NaCl),[76] most hydrogels,[78,96] and some nanomaterials (e.g., Au nanoparticles, graphene, etc.) have proven to be bio-compatible.[91] Second, non-bio-compatible materials can be coated with bio-compatible materials or encapsulations. For example, AgNWs can be coated with Au to enhance bio-compatibility.[111] Synthetic polymers, such as PDMS,[180] poly(EG) (PEG), and PVA, have been widely used as bio-compatible encapsulation layers to insulate non-bio-compatible devices.[181]

With so many exciting opportunities in fundamental and applied research, the future of body-conformable electronics is wide and bright. We expect intrinsically soft organic semiconductors, soft active materials, origami and bio-inspired designs, 3D printing, and multiphysics interface modeling to play more significant roles in body-conformable electronics in the years to come.

ACKNOWLEDGMENTS

The authors of this review article are supported partially by the U.S. Office of Naval Research under grant N00014-20-1-2112, the US Army Research Office under Cooperative Agreement W911NF-19-2-0333, and the US National Science Foundation under grants 1738293 and 2133106. The views and conclusions contained in this review are those of the authors and should not be interpreted as representing the official policies, either expressed or implied, of the US Office of Naval Research, the US Army Research Office, the US National Science Foundation, or the US government.

DECLARATION OF INTERESTS

The authors declare no competing interests.

REFERENCES

1. Rao, Z., Ershad, F., Almasri, A., Gonzalez, L., Wu, X., and Yu, C. (2020). Soft electronics for the skin: from health monitors to human–machine interfaces. Adv. Mater. Tech. *5*, 2000233. https://doi.org/10.1002/admt.202000233.

2. Norton, J.J.S., Lee, D.S., Lee, J.W., Lee, W., Kwon, O., Won, P., Jung, S.-Y., Cheng, H., Jeong, J.-W., Akce, A., et al. (2015). Soft, curved electrode systems capable of integration on the auricle as a persistent brain–computer interface. Proc. Natl. Acad. Sci. U S A *112*, 3920–3925. https://doi.org/10.1073/pnas.1424875112.

3. Ha, T., Tran, J., Liu, S., Jang, H., Jeong, H., Mitbander, R., Huh, H., Qiu, Y., Duong, J., Wang, R.L., et al. (2019). A chest-laminated ultrathin and stretchable E-tattoo for the measurement of electrocardiogram, seismocardiogram, and cardiac time intervals. Adv. Sci. (Weinh) *6*, 1900290. https://doi.org/10.1002/advs.201900290.

4. Wang, Y., Yin, L., Bai, Y., Liu, S., Wang, L., Zhou, Y., Hou, C., Yang, Z., Wu, H., Ma, J., et al. (2020). Electrically compensated, tattoo-like electrodes for epidermal electrophysiology at scale. Sci. Adv. *6*, eabd0996. https://doi.org/10.1126/sciadv.abd0996.

5. Kim, D.H., Lu, N., Ma, R., Kim, Y.S., Kim, R.H., Wang, S., Wu, J., Won, S.M., Tao, H., Islam, A., et al. (2011). Epidermal electronics. Science *333*, 838–843. https://doi.org/10.1126/science.1206157.

6. Hong, Y.J., Jeong, H., Cho, K.W., Lu, N., and Kim, D.H. (2019). Wearable and implantable devices for cardiovascular healthcare: from monitoring to therapy based on flexible and stretchable electronics. Adv. Funct. Mater. *29*, 1808247. https://doi.org/10.1002/adfm.201808247.

7. Kim, M.K., Parasuraman, R.N., Wang, L., Park, Y., Kim, B., Lee, S.J., Lu, N., Min, B.-C., and Lee, C.H. (2019). Soft-packaged sensory glove system for human-like natural interaction and control of prosthetic hands. NPG Asia Mater. *11*, 1–12. https://doi.org/10.1038/s41427-019-0143-9.

8. Barr, A. (2014). Google Developing Smart Contact Lens (USA Today). https://www.usatoday.com/story/tech/2014/01/16/google-smart-contact-lens/4540727/.

9. Gao, W., Emaminejad, S., Nyein, H.Y.Y., Challa, S., Chen, K., Peck, A., Fahad, H.M., Ota, H., Shiraki, H., Kiriya, D., et al. (2016). Fully integrated wearable sensor arrays for multiplexed in situ perspiration analysis. Nature *529*, 509–514. https://doi.org/10.1038/nature16521.

10. Han, M., Wang, H., Yang, Y., Liang, C., Bai, W., Yan, Z., Li, H., Xue, Y., Wang, X., Akar, B., et al. (2019). Three-dimensional piezoelectric polymer microsystems for vibrational energy harvesting, robotic interfaces and biomedical implants. Nat. Electron. *2*, 26–35. https://doi.org/10.1038/s41928-018-0189-7.

11. Khan, M.B., Kim, D.H., Han, J.H., Saif, H., Lee, H., Lee, Y., Kim, M., Jang, E., Hong, S.K., Joe, D.J., et al. (2019). Performance improvement of flexible piezoelectric energy harvester for irregular human motion with energy extraction enhancement circuit. Nano Energy *58*, 211–219. https://doi.org/10.1016/j.nanoen.2019.01.049.

12. Minev, I.R., Musienko, P., Hirsch, A., Barraud, Q., Wenger, N., Moraud, E.M., Gandar, J., Capogrosso, M., Milekovic, T., Asboth, L., et al. (2015). Electronic dura mater for long-term multimodal neural interfaces. Science *347*, 159–163. https://doi.org/10.1126/science.1260318.

13. Park, S.I., Shin, G., McCall, J.G., Al-Hasani, R., Norris, A., Xia, L., Brenner, D.S., Noh, K.N., Bang, S.Y., Bhatti, D.L., et al. (2016). Stretchable multichannel antennas in soft wireless optoelectronic implants for optogenetics. Proc. Natl. Acad. Sci. U S A *113*, E8169–E8177. https://doi.org/10.1073/pnas.1611769113.

14. Choi, C., Choi, M.K., Liu, S., Kim, M.S., Park, O.K., Im, C., Kim, J., Qin, X., Lee, G.J., Cho, K.W., et al. (2017). Human eye-inspired soft optoelectronic device using high-density MoS_2-graphene curved image sensor array. Nat. Commun. *8*, 1–11. https://doi.org/10.1038/s41467-017-01824-6.

15. Kim, J., Lee, M., Shim, H.J., Ghaffari, R., Cho, H.R., Son, D., Jung, Y.H., Soh, M., Choi, C., Jung, S., et al. (2014). Stretchable silicon nanoribbon electronics for skin prosthesis. Nat. Commun. *5*, 5747. https://doi.org/10.1038/ncomms6747.

16. Jeong, J.W., Yeo, W.H., Akhtar, A., Norton, J.J., Kwack, Y.J., Li, S., Jung, S.Y., Su, Y., Lee, W., Xia, J., et al. (2013). Materials and optimized designs for human-machine interfaces via epidermal electronics. Adv. Mater. *25*, 6839–6846. https://doi.org/10.1002/adma.201301921.

17. Kabiri Ameri, S., Ho, R., Jang, H., Tao, L., Wang, Y., Wang, L., Schnyer, D.M., Akinwande, D., and Lu, N. (2017). Graphene electronic tattoo sensors. ACS Nano *11*, 7634–7641. https://doi.org/10.1021/acsnano.7b02182.

18. Ershad, F., Thukral, A., Yue, J., Comeaux, P., Lu, Y., Shim, H., Sim, K., Kim, N.I., Rao, Z., Guevara, R., et al. (2020). Ultra-conformal drawn-on-skin electronics for multifunctional motion artifact-free sensing and point-of-care treatment. Nat. Commun. *11*, 3823. https://doi.org/10.1038/s41467-020-17619-1.

19. Webster, J.G. (1984). Reducing motion artifacts and interference in biopotential recording. IEEE Trans. Biomed. Eng. *31*, 823–826. https://doi.org/10.1109/TBME.1984.325244.

20. Li, H., Liu, H., Sun, M., Huang, Y., and Xu, L. (2021). 3D interfacing between soft electronic tools and complex biological tissues. Adv. Mater. *33*, 2004425. https://doi.org/10.1002/adma.202004425.

21. Sunwoo, S.H., Ha, K.H., Lee, S., Lu, N., and Kim, D.H. (2021). Wearable and implantable soft bioelectronics: device designs and material strategies. Annu. Rev. Chem. Biomol. Eng. *12*, 359–391. https://doi.org/10.1146/annurev-chembioeng-101420-024336.

22. Chiong, J.A., Tran, H., Lin, Y., Zheng, Y., and Bao, Z. (2021). Integrating emerging polymer chemistries for the advancement of recyclable, biodegradable, and biocompatible electronics. Adv. Sci. (Weinh) *8*, e2101233. https://doi.org/10.1002/advs.202101233.

23. Mannoor, M.S., Tao, H., Clayton, J.D., Sengupta, A., Kaplan, D.L., Naik, R.R., Verma, N., Omenetto, F.G., and McAlpine, M.C. (2012). Graphene-based wireless bacteria detection on tooth enamel. Nat. Commun. *3*, 763. https://doi.org/10.1038/ncomms1767.

24. Jeong, H., Wang, L., Ha, T., Mitbander, R., Yang, X., Dai, Z., Qiao, S., Shen, L., Sun, N., and Lu, N. (2019). Modular and reconfigurable wireless E-tattoos for personalized sensing. Adv. Mater. Tech. *4*, 1900117. https://doi.org/10.1002/admt.201900117.

25. Huang, X., Cheng, H., Chen, K., Zhang, Y., Zhang, Y., Liu, Y., Zhu, C., Ouyang, S.C., Kong, G.W., Yu, C., et al. (2013). Epidermal impedance sensing sheets for precision hydration assessment and spatial mapping. IEEE Trans. Biomed. Eng. *60*, 2848–2857. https://doi.org/10.1109/TBME.2013.2264879.

26. Xu, L., Gutbrod, S.R., Ma, Y., Petrossians, A., Liu, Y., Webb, R.C., Fan, J.A., Yang, Z., Xu, R., Whalen, J.J., 3rd, et al. (2015). Materials and fractal designs for 3D multifunctional integumentary membranes with capabilities in cardiac electrotherapy. Adv. Mater. *27*, 1731–1737. https://doi.org/10.1002/adma.201405017.

27. Ameri, S.K., Kim, M., Kuang, I.A., Perera, W.K., Alshiekh, M., Jeong, H., Topcu, U., Akinwande, D., and Lu, N. (2018). Imperceptible electrooculography graphene sensor system for human–robot interface. npj 2D Mater. Appl. *2*, 1–7. https://doi.org/10.1038/s41699-018-0064-4.

28. Chen, X., Assadsangabi, B., Hsiang, Y., and Takahata, K. (2018). Enabling angioplasty-ready "Smart" stents to detect in-stent restenosis and occlusion. Adv. Sci. *5*, 1700560. https://doi.org/10.1002/advs.201700560.

29. Zhang, Y., Zheng, N., Cao, Y., Wang, F., Wang, P., Ma, Y., Lu, B., Hou, G., Fang, Z., Liang, Z., et al. (2019). Climbing-inspired twining electrodes using shape memory for peripheral nerve stimulation and recording. Sci. Adv. *5*, eaaw1066. https://doi.org/10.1126/sciadv.aaw1066.

30. Tang, L., Shang, J., and Jiang, X. (2021). Multilayered electronic transfer tattoo that can enable the crease amplification effect. Sci. Adv. *7*, eabe3778. https://doi.org/10.1126/sciadv.abe3778.

31. Mao, S.S., Ahmadi, N., Shah, B., Beckmann, D., Chen, A., Ngo, L., Flores, F.R., Gao, Y.L., and Budoff, M.J. (2008). Normal thoracic aorta diameter on cardiac computed tomography in healthy asymptomatic adults: impact of age and gender. Acad. Radiol. *15*, 827–834. https://doi.org/10.1016/j.acra.2008.02.001.

32. Bekerman, I., Gottlieb, P., and Vaiman, M. (2014). Variations in eyeball diameters of the

healthy adults. J. Ophthalmol. *2014*, 503645. https://doi.org/10.1155/2014/503645.

33. Simon, G., Reid, L., Tanner, J., Goldstein, H., and Benjamin, B. (1972). Growth of radiologically determined heart diameter, lung width, and lung length from 5-19 years, with standards for clinical use. Arch. Dis. Child. *47*, 373–381. https://doi.org/10.1136/adc.47.253.373.

34. Burton, H.E., Cullinan, R., Jiang, K., and Espino, D.M. (2019). Multiscale three-dimensional surface reconstruction and surface roughness of porcine left anterior descending coronary arteries. R. Soc. Open Sci. *6*, 190915. https://doi.org/10.1098/rsos.190915.

35. Tchvialeva, L., Zeng, H., Markhvida, I., McLean, D.I., Lui, H., and Lee, T.K. (2010). Skin roughness assessment. N. Dev. Biomed. Eng. 341–358. https://doi.org/10.5772/7611.

36. Fan, J.A., Yeo, W.H., Su, Y., Hattori, Y., Lee, W., Jung, S.Y., Zhang, Y., Liu, Z., Cheng, H., Falgout, L., et al. (2014). Fractal design concepts for stretchable electronics. Nat. Commun. *5*, 3266. https://doi.org/10.1038/ncomms4266.

37. Wang, S., Xu, J., Wang, W., Wang, G.N., Rastak, R., Molina-Lopez, F., Chung, J.W., Niu, S., Feig, V.R., Lopez, J., et al. (2018). Skin electronics from scalable fabrication of an intrinsically stretchable transistor array. Nature *555*, 83–88. https://doi.org/10.1038/nature25494.

38. Xu, L., Gutbrod, S.R., Bonifas, A.P., Su, Y., Sulkin, M.S., Lu, N., Chung, H.J., Jang, K.I., Liu, Z., Ying, M., et al. (2014). 3D multifunctional integumentary membranes for spatiotemporal cardiac measurements and stimulation across the entire epicardium. Nat. Commun. *5*, 3329. https://doi.org/10.1038/ncomms4329.

39. Miyamoto, A., Lee, S., Cooray, N.F., Lee, S., Mori, M., Matsuhisa, N., Jin, H., Yoda, L., Yokota, T., Itoh, A., et al. (2017). Inflammation-free, gas-permeable, lightweight, stretchable on-skin electronics with nanomeshes. Nat. Nanotechnol. *12*, 907–913. https://doi.org/10.1038/nnano.2017.125.

40. Chen, Y.C., and Yang, H. (2017). Octopus-inspired assembly of nanosucker arrays for dry/wet adhesion. ACS Nano *11*, 5332–5338. https://doi.org/10.1021/acsnano.7b00809.

41. Hwang, I., Kim, H.N., Seong, M., Lee, S.H., Kang, M., Yi, H., Bae, W.G., Kwak, M.K., and Jeong, H.E. (2018). Multifunctional smart skin adhesive patches for advanced health care. Adv. Healthc. Mater. *7*, e1800275. https://doi.org/10.1002/adhm.201800275.

42. Liu, J., Zheng, H., Poh, P.S., Machens, H.G., and Schilling, A.F. (2015). Hydrogels for engineering of perfusable vascular networks. Int. J. Mol. Sci. *16*, 15997–16016. https://doi.org/10.3390/ijms160715997.

43. Saveleva, M.S., Eftekhari, K., Abalymov, A., Douglas, T.E., Volodkin, D., Parakhonskiy, B.V., and Skirtach, A.G. (2019). Hierarchy of hybrid materials—the place of inorganics-in-organics in it, their composition and applications. Front. Chem. *7*, 179. https://doi.org/10.3389/fchem.2019.00179.

44. Lang, U., and .Dual, J., eds. Mechanical properties of the intrinsically conductive polymer poly (3, 4-ethylenedioxythiophene) poly (styrenesulfonate)(PEDOT/PSS). In Key Engineering Materials (Trans Tech Publ), pp. 1189–1192.

45. Tahk, D., Lee, H.H., and Khang, D.-Y. (2009). Elastic moduli of organic electronic materials by the buckling method. Macromolecules *42*, 7079–7083. https://doi.org/10.1021/ma900137k.

46. Ozawa, H., Matsumoto, T., Ohashi, T., Sato, M., and Kokubun, S. (2001). Comparison of spinal cord gray matter and white matter softness: measurement by pipette aspiration method. J. Neurosurg. *95*, 221–224. https://doi.org/10.3171/spi.2001.95.2.0221.

47. Kalra, A., Lowe, A., and Al-Jumaily, A. (2016). Mechanical behaviour of skin: a review. J. Mater. Sci. Eng. *5*, 1000254. https://doi.org/10.1177/0954411918759801.

48. Christensen, M.B., Pearce, S.M., Ledbetter, N.M., Warren, D.J., Clark, G.A., and Tresco, P.A. (2014). The foreign body response to the Utah Slant Electrode Array in the cat sciatic nerve. Acta Biomater. *10*, 4650–4660. https://doi.org/10.1016/j.actbio.2014.07.010.

49. Garcia-Sandoval, A., Pal, A., Mishra, A.M., Sherman, S., Parikh, A.R., Joshi-Imre, A., Arreaga-Salas, D., Gutierrez-Heredia, G., Duran-Martinez, A.C., Nathan, J., et al. (2018). Chronic softening spinal cord stimulation arrays. J. Neural Eng. *15*, 045002. https://doi.org/10.1088/1741-2552/aab90d.

50. Tian, Z., Zhao, Y., Wang, S., Zhou, G., Zhao, N., and Wong, C.-P. (2020). A highly stretchable and conductive composite based on an emulsion-templated silver nanowire aerogel. J. Mater. Chem. A *8*, 1724–1730. https://doi.org/10.1039/C9TA11225A.

51. Amjadi, M., Yoon, Y.J., and Park, I. (2015). Ultra-stretchable and skin-mountable strain sensors using carbon nanotubes–Ecoflex nanocomposites. Nanotechnology *26*, 375501. https://doi.org/10.1088/0957-4484/26/37/375501.

52. Aletras, A.H., Balaban, R.S., and Wen, H. (1999). High-resolution strain analysis of the human heart with fast-DENSE. J. Magn. Reson. *140*, 41–57. https://doi.org/10.1006/jmre.1999.1821.

53. Sabet, A.A., Christoforou, E., Zatlin, B., Genin, G.M., and Bayly, P.V. (2008). Deformation of the human brain induced by mild angular head acceleration. J. Biomech. *41*, 307–315. https://doi.org/10.1016/j.jbiomech.2007.09.016.

54. Guan, Y.S., Thukral, A., Zhang, S., Sim, K., Wang, X., Zhang, Y., Ershad, F., Rao, Z., Pan, F., Wang, P., et al. (2020). Air/water interfacial assembled rubbery semiconducting nanofilm for fully rubbery integrated electronics. Sci. Adv. *6*, eabb3656. https://doi.org/10.1126/sciadv.abb3656.

55. Lv, G., Wang, H., Tong, Y., Dong, L., Zhao, X., Zhao, P., Tang, Q., and Liu, Y. (2020). Flexible, conformable organic semiconductor proximity sensor array for electronic skin. Adv. Mater. Inter. *7*, 2000306. https://doi.org/10.1002/admi.202000306.

56. Kim, D.C., Shim, H.J., Lee, W., Koo, J.H., and Kim, D.H. (2020). Material-based approaches for the fabrication of stretchable electronics. Adv. Mater. *32*, e1902743. https://doi.org/10.1002/adma.201902743.

57. Wang, C., Wang, C., Huang, Z., and Xu, S. (2018). Materials and structures toward soft electronics. Adv. Mater. *30*, e1801368. https://doi.org/10.1002/adma.201801368.

58. Zhang, Y. (2016). Mechanics and designs of stretchable bioelectronics. Stretchable Bioelectron. Med. Dev. Syst. 53–68. https://doi.org/10.1007/978-3-319-28694-5_3.

59. Bae, W.G., Kim, D., Kwak, M.K., Ha, L., Kang, S.M., and Suh, K.Y. (2013). Enhanced skin adhesive patch with modulus-tunable composite micropillars. Adv. Healthc. Mater. *2*, 109–113. https://doi.org/10.1002/adhm.201200098.

60. Pang, C., Koo, J.H., Nguyen, A., Caves, J.M., Kim, M.G., Chortos, A., Kim, K., Wang, P.J., Tok, J.B., and Bao, Z. (2015). Highly skin-conformal microhairy sensor for pulse signal amplification. Adv. Mater. *27*, 634–640. https://doi.org/10.1002/adma.201403807.

61. Li, J., Celiz, A.D., Yang, J., Yang, Q., Wamala, I., Whyte, W., Seo, B.R., Vasilyev, N.V., Vlassak, J.J., Suo, Z., et al. (2017). Tough adhesives for diverse wet surfaces. Science *357*, 378–381. https://doi.org/10.1126/science.aah6362.

62. Deng, J., Yuk, H., Wu, J., Varela, C.E., Chen, X., Roche, E.T., Guo, C.F., and Zhao, X. (2021). Electrical bioadhesive interface for bioelectronics. Nat. Mater. *20*, 229–236. https://doi.org/10.1038/s41563-020-00814-2.

63. Kim, D.H., Viventi, J., Amsden, J.J., Xiao, J., Vigeland, L., Kim, Y.S., Blanco, J.A., Panilaitis, B., Frechette, E.S., Contreras, D., et al. (2010). Dissolvable films of silk fibroin for ultrathin conformal bio-integrated electronics. Nat. Mater. *9*, 511–517. https://doi.org/10.1038/nmat2745.

64. Wang, L., and Lu, N. (2016). Conformability of a thin elastic membrane laminated on a soft substrate with slightly wavy surface. J. Appl. Mech. *83*. https://doi.org/10.1115/1.4032466.

65. Wang, L., Qiao, S., Kabiri Ameri, S., Jeong, H., and Lu, N. (2017). A thin elastic membrane conformed to a soft and rough substrate subjected to stretching/compression. J. Appl. Mech. *84*. https://doi.org/10.1115/1.4037740.

66. Wang, S., Li, M., Wu, J., Kim, D.-H., Lu, N., Su, Y., Kang, Z., Huang, Y., and Rogers, J.A. (2012). Mechanics of epidermal electronics. J. Appl. Mech. *79*. https://doi.org/10.1115/1.4005963.

67. Li, L., Lin, H., Qiao, S., Zou, Y., Danto, S., Richardson, K., Musgraves, J.D., Lu, N., and Hu, J. (2014). Integrated flexible chalcogenide glass photonic devices. Nat. Photon. *8*, 643–649. https://doi.org/10.1038/nphoton.2014.138.

68. Li, S., Su, Y., and Li, R. (2016). Splitting of the neutral mechanical plane depends on the length of the multi-layer structure of flexible electronics. Proc. Math. Phys. Eng. Sci. *472*, 20160087. https://doi.org/10.1098/rspa.2016.0087.

69. Ameri, S., .Ho, R., .Jang, H., .Wang, Y., .Schnyer, D., .Akinwande, D., and .Lu, N., eds. Thinnest transparent epidermal sensor system based on graphene. In 2016 IEEE International Electron Devices Meeting (IEDM) (IEEE), pp. 18.4.1–18.4.4.

70. Baik, S., Lee, H.J., Kim, D.W., Min, H., and Pang, C. (2019). Capillarity-enhanced organ-attachable adhesive with highly drainable wrinkled octopus-inspired architectures. ACS Appl. Mater. Inter. *11*, 25674–25681. https://doi.org/10.1021/acsami.9b05511.

71. Zhang, L., Kumar, K.S., He, H., Cai, C.J., He, X., Gao, H., Yue, S., Li, C., Seet, R.C., Ren, H., et al. (2020). Fully organic compliant dry electrodes self-adhesive to skin for long-term motion-robust epidermal biopotential monitoring. Nat. Commun. *11*, 4683. https://doi.org/10.1038/s41467-020-18503-8.

72. Trung, T.Q., and Lee, N.E. (2017). Recent progress on stretchable electronic devices with intrinsically stretchable components. Adv. Mater. *29*, 1603167. https://doi.org/10.1002/adma.201603167.

73. Sim, K., Rao, Z., Ershad, F., and Yu, C. (2020). Rubbery electronics fully made of stretchable elastomeric electronic materials. Adv. Mater. *32*, 1902417. https://doi.org/10.1002/adma.201902417.

74. Gui, Q., He, Y., and Wang, Y. (2021). Soft electronics based on liquid conductors. Adv. Electron. Mater. *7*, 2000780. https://doi.org/10.1002/aelm.202000780.

75. Park, Y.G., Lee, G.Y., Jang, J., Yun, S.M., Kim, E., and Park, J.U. (2021). Liquid metal-based soft electronics for wearable healthcare. Adv. Healthc. Mater. *10*, e2002280. https://doi.org/10.1002/adhm.202002280.

76. Choi, D.Y., Kim, M.H., Oh, Y.S., Jung, S.H., Jung, J.H., Sung, H.J., Lee, H.W., and Lee, H.M. (2017). Highly stretchable, hysteresis-free ionic liquid-based strain sensor for precise human motion monitoring. ACS Appl. Mater. Inter. *9*, 1770–1780. https://doi.org/10.1021/acsami.6b12415.

77. Liao, M., Wan, P., Wen, J., Gong, M., Wu, X., Wang, Y., Shi, R., and Zhang, L. (2017). Wearable, healable, and adhesive epidermal sensors assembled from mussel-inspired conductive hybrid hydrogel framework. Adv. Funct. Mater. *27*, 1703852. https://doi.org/10.1002/adfm.201703852.

78. Sun, X., Yao, F., and Li, J. (2020). Nanocomposite hydrogel-based strain and pressure sensors: a review. J. Mater. Chem. A *8*, 18605–18623. https://doi.org/10.1039/D0TA06965E.

79. Peng, B., Zhao, F., Ping, J., and Ying, Y. (2020). Recent advances in nanomaterial-enabled wearable sensors: material synthesis, sensor design, and personal health monitoring. Small *16*, e2002681. https://doi.org/10.1002/smll.202002681.

80. Tavakoli, M., Malakooti, M.H., Paisana, H., Ohm, Y., Marques, D.G., Alhais Lopes, P., Piedade, A.P., de Almeida, A.T., and Majidi, C. (2018). EGaIn-assisted room-temperature sintering of silver nanoparticles for stretchable, inkjet-printed, thin-film electronics. Adv. Mater. *30*, e1801852. https://doi.org/10.1002/adma.201801852.

81. Zhu, G.J., Ren, P.G., Guo, H., Jin, Y.L., Yan, D.X., and Li, Z.M. (2019). Highly sensitive and stretchable polyurethane fiber strain sensors with embedded silver nanowires. ACS Appl. Mater. Inter. *11*, 23649–23658. https://doi.org/10.1021/acsami.9b08611.

82. Chun, S., Son, W., Kim, D.W., Lee, J., Min, H., Jung, H., Kwon, D., Kim, A.H., Kim, Y.-J., Lim, S.K., et al. (2019). Water-resistant and skin-adhesive wearable electronics using graphene fabric sensor with octopus-inspired microsuckers. ACS Appl. Mater. Inter. *11*, 16951–16957. https://doi.org/10.1021/acsami.9b04206.

83. Tao, L.Q., Tian, H., Liu, Y., Ju, Z.Y., Pang, Y., Chen, Y.Q., Wang, D.Y., Tian, X.G., Yan, J.C., Deng, N.Q., et al. (2017). An intelligent artificial throat with sound-sensing ability based on laser induced graphene. Nat. Commun. *8*, 14579. https://doi.org/10.1038/ncomms14579.

84. Li, J., Shi, Q., Röhr, J.A., Wu, H., Wu, B., Guo, Y., Zhang, Q., Hou, C., Li, Y., and Wang, H. (2020). Flexible 3D porous MoS2/CNTs architectures with ZT of 0.17 at room temperature for wearable thermoelectric applications. Adv. Funct. Mater. *30*, 2002508. https://doi.org/10.1002/adfm.202002508.

85. Chan, K.H., and So, S.-K. (2011). Using admittance spectroscopy to quantify transport properties of P3HT thin films. J. Photon. Energy *1*, 011112. https://doi.org/10.1117/1.3556727.

86. Lazarus, N., Meyer, C., Bedair, S., Nochetto, H., and Kierzewski, I. (2014). Multilayer liquid metal stretchable inductors. Smart Mater. Struct. *23*, 085036. https://doi.org/10.1088/0964-1726/23/8/085036.

87. Lipomi, D.J., Vosgueritchian, M., Tee, B.C., Hellstrom, S.L., Lee, J.A., Fox, C.H., and Bao, Z. (2011). Skin-like pressure and strain sensors based on transparent elastic films of carbon nanotubes. Nat. Nanotechnol. *6*, 788–792. https://doi.org/10.1038/nnano.2011.184.

88. Le Floch, P., Molinari, N., Nan, K., Zhang, S., Kozinsky, B., Suo, Z., and Liu, J. (2020). Fundamental limits to the electrochemical impedance stability of dielectric elastomers in bioelectronics. Nano Lett. *20*, 224–233. https://doi.org/10.1021/acs.nanolett.9b03705.

89. Yao, S., Ren, P., Song, R., Liu, Y., Huang, Q., Dong, J., O'Connor, B.T., and Zhu, Y. (2020). Nanomaterial-enabled flexible and stretchable sensing systems: processing, integration, and applications. Adv. Mater. *32*, e1902343. https://doi.org/10.1002/adma.201902343.

90. Lee, W., Yun, H., Song, J.-K., Sunwoo, S.-H., and Kim, D.-H. (2021). Nanoscale materials and deformable device designs for bioinspired and biointegrated electronics. Acc. Mater. Res. *2*, 266–281. https://doi.org/10.1021/accountsmr.1c00020.

91. Wang, C., Xia, K., Wang, H., Liang, X., Yin, Z., and Zhang, Y. (2019). Advanced carbon for flexible and wearable electronics. Adv. Mater. *31*, e1801072. https://doi.org/10.1002/adma.201801072.

92. Wang, S., Fang, Y., He, H., Zhang, L., Li, C.A., and Ouyang, J. (2021). Wearable stretchable dry and self-adhesive strain sensors with conformal contact to skin for high-quality motion monitoring. Adv. Funct. Mater. *31*, 2007495. https://doi.org/10.1002/adfm.202007495.

93. Zhang, P., Ma, L., Fan, F., Zeng, Z., Peng, C., Loya, P.E., Liu, Z., Gong, Y., Zhang, J., Zhang, X., et al. (2014). Fracture toughness of graphene. Nat. Commun. *5*, 3782. https://doi.org/10.1038/ncomms4782.

94. Kim, N., Kee, S., Lee, S.H., Lee, B.H., Kahng, Y.H., Jo, Y.R., Kim, B.J., and Lee, K. (2014). Highly conductive PEDOT:PSS nanofibrils induced by solution-processed crystallization. Adv. Mater. *26*, 2268–2272. https://doi.org/10.1002/adma.201304611.

95. Lang, U., Naujoks, N., and Dual, J. (2009). Mechanical characterization of PEDOT: PSS thin films. Synth. Met. *159*, 473–479. https://doi.org/10.1016/j.synthmet.2008.11.005.

96. Ray, T.R., Choi, J., Bandodkar, A.J., Krishnan, S., Gutruf, P., Tian, L., Ghaffari, R., and Rogers, J.A. (2019). Bio-integrated wearable systems: a comprehensive review. Chem. Rev. *119*, 5461–5533. https://doi.org/10.1021/acs.chemrev.8b00573.

97. Won, P., Jeong, S., Majidi, C., and Ko, S.H. (2021). Recent advances in liquid-metal-based wearable electronics and materials. iScience *24*, 102698. https://doi.org/10.1016/j.isci.2021.102698.

98. Ko, H.C., Stoykovich, M.P., Song, J., Malyarchuk, V., Choi, W.M., Yu, C.J., Geddes, J.B., 3rd, Xiao, J., Wang, S., Huang, Y., et al. (2008). A hemispherical electronic eye camera based on compressible silicon optoelectronics. Nature *454*, 748–753. https://doi.org/10.1038/nature07113.

99. Jones, J., Lacour, S.P., Wagner, S., and Suo, Z. (2004). Stretchable wavy metal interconnects. J. Vacuum Sci. Technol. A Vacuum Surf. Films *22*, 1723–1725. https://doi.org/10.1116/1.1756879.

100. Khang, D.Y., Jiang, H., Huang, Y., and Rogers, J.A. (2006). A stretchable form of single-crystal silicon for high-performance electronics on rubber substrates. Science *311*, 208–212. https://doi.org/10.1126/science.1121401.

101. Wang, X., Feiner, R., Luan, H., Zhang, Q., Zhao, S., Zhang, Y., Han, M., Li, Y., Sun, R., Wang, H., et al. (2020). Three-dimensional electronic scaffolds for monitoring and regulation of multifunctional hybrid tissues. Extreme Mech. Lett. *35*, 100634. https://doi.org/10.1016/j.eml.2020.100634.

102. Park, G., Chung, H.J., Kim, K., Lim, S.A., Kim, J., Kim, Y.S., Liu, Y., Yeo, W.H., Kim, R.H., Kim, S.S., et al. (2014). Immunologic and tissue biocompatibility of flexible/stretchable electronics and optoelectronics. Adv. Healthc. Mater. *3*, 515–525. https://doi.org/10.1002/adhm.201300220.

103. Gray, D.S., Tien, J., and Chen, C.S. (2004). High-conductivity elastomeric electronics. Adv. Mater. *16*, 393–397. https://doi.org/10.1002/adma.200306107.

104. Li, T., Suo, Z., Lacour, S.P., and Wagner, S. (2005). Compliant thin film patterns of stiff materials as platforms for stretchable electronics. J. Mater. Res. *20*, 3274–3277. https://doi.org/10.1557/jmr.2005.0422.

105. Zhang, Y., Xu, S., Fu, H., Lee, J., Su, J., Hwang, K.C., Rogers, J.A., and Huang, Y. (2013). Buckling in serpentine microstructures and applications in elastomer-supported ultra-stretchable electronics with high areal coverage. Soft Matter *9*, 8062–8070. https://doi.org/10.1039/C3SM51360B.

106. Yang, S., Qiao, S., and Lu, N. (2017). Elasticity solutions to nonbuckling serpentine ribbons. J. Appl. Mech. *84*, 021004. https://doi.org/10.1115/1.4035118.

107. Lu, N., and Yang, S. (2015). Mechanics for stretchable sensors. Curr. Opin. Solid State Mater. Sci. *19*, 149–159. https://doi.org/10.1016/j.cossms.2014.12.007.

108. Xu, S., Zhang, Y., Cho, J., Lee, J., Huang, X., Jia, L., Fan, J.A., Su, Y., Su, J., Zhang, H., et al. (2013). Stretchable batteries with self-similar serpentine interconnects and integrated wireless recharging systems. Nat. Commun. *4*, 1543. https://doi.org/10.1038/ncomms2553.

109. Xiao, L., Zhu, C., Xiong, W., Huang, Y., and Yin, Z. (2018). The conformal design of an island-bridge structure on a non-developable surface for stretchable electronics. Micromachines (Basel) *9*, 392. https://doi.org/10.3390/mi9080392.

110. Liu, S., Ha, T., and Lu, N. (2019). Experimentally and numerically validated analytical solutions to nonbuckling piezoelectric serpentine ribbons. J. Appl. Mech. *86*. https://doi.org/10.1115/1.4042570.

111. Choi, S., Han, S.I., Jung, D., Hwang, H.J., Lim, C., Bae, S., Park, O.K., Tschabrunn, C.M., Lee, M., Bae, S.Y., et al. (2018). Highly conductive, stretchable and biocompatible Ag–Au core–sheath nanowire composite for wearable and implantable bioelectronics. Nat. Nanotechnol. *13*, 1048–1056. https://doi.org/10.1038/s41565-018-0226-8.

112. Li, L., Lin, H., Qiao, S., Huang, Y.Z., Li, J.Y., Michon, J., Gu, T., Alosno-Ramos, C., Vivien, L., Yadav, A., et al. (2018). Monolithically integrated stretchable photonics. Light Sci. Appl. *7*, 17138. https://doi.org/10.1038/lsa.2017.138.

113. Jang, K.I., Chung, H.U., Xu, S., Lee, C.H., Luan, H., Jeong, J., Cheng, H., Kim, G.T., Han, S.Y., Lee, J.W., et al. (2015). Soft network composite materials with deterministic and bio-inspired designs. Nat. Commun. *6*, 6566. https://doi.org/10.1038/ncomms7566.

114. Morikawa, Y., Yamagiwa, S., Sawahata, H., Numano, R., Koida, K., Ishida, M., and Kawano, T. (2018). Ultrastretchable kirigami bioprobes. Adv. Healthc. Mater. *7*, 1701100. https://doi.org/10.1002/adhm.201701100.

115. Zhong, J., Zhang, Y., Zhong, Q., Hu, Q., Hu, B., Wang, Z.L., and Zhou, J. (2014). Fiber-based generator for wearable electronics and mobile medication. ACS Nano *8*, 6273–6280. https://doi.org/10.1021/nn501732z.

116. Zhang, Y., Fu, H., Su, Y., Xu, S., Cheng, H., Fan, J.A., Hwang, K.-C., Rogers, J.A., and Huang, Y. (2013). Mechanics of ultra-stretchable self-similar serpentine interconnects. Acta Mater. *61*, 7816–7827. https://doi.org/10.1016/j.actamat.2013.09.020.

117. Lee, W., Kobayashi, S., Nagase, M., Jimbo, Y., Saito, I., Inoue, Y., Yambe, T., Sekino, M., Malliaras, G.G., Yokota, T., et al. (2018). Nonthrombogenic, stretchable, active multielectrode array for electroanatomical mapping. Sci. Adv. *4*, eaau2426. https://doi.org/10.1126/sciadv.aau2426.

118. Li, H., Ma, Y., Liang, Z., Wang, Z., Cao, Y., Xu, Y., Zhou, H., Lu, B., Chen, Y., Han, Z., et al. (2020). Wearable skin-like optoelectronic systems with suppression of motion artifacts for cuff-less continuous blood pressure monitor. Natl. Sci. Rev. *7*, 849–862. https://doi.org/10.1093/nsr/nwaa022.

119. Matsuhisa, N., Chen, X., Bao, Z., and Someya, T. (2019). Materials and structural designs of stretchable conductors. Chem. Soc. Rev. *48*, 2946–2966. https://doi.org/10.1039/c8cs00814k.

120. Gao, J., Shang, K., Ding, Y., and Wen, Z. (2021). Material and configuration design strategies towards flexible and wearable power supply devices: a review. J. Mater. Chem. A *9*, 8950–8965. https://doi.org/10.1039/D0TA11260G.

121. Morikawa, Y., Yamagiwa, S., Sawahata, H., Numano, R., Koida, K., and Kawano, T. (2019). Donut-shaped stretchable kirigami: enabling electronics to integrate with the deformable muscle. Adv. Healthc. Mater. *8*, e1900939. https://doi.org/10.1002/adhm.201900939.

122. Sun, R., Carreira, S.C., Chen, Y., Xiang, C., Xu, L., Zhang, B., Chen, M., Farrow, I., Scarpa, F., and Rossiter, J. (2019). Stretchable piezoelectric sensing systems for self-powered and wireless health monitoring. Adv. Mater. Tech. *4*, 1900100. https://doi.org/10.1002/admt.201900100.

123. Xu, X., Xie, S., Zhang, Y., and Peng, H. (2019). The rise of fiber electronics. Angew. Chem. Int. Ed. Engl. *58*, 13643–13653. https://doi.org/10.1002/anie.201902425.

124. Lee, J., Kwon, H., Seo, J., Shin, S., Koo, J.H., Pang, C., Son, S., Kim, J.H., Jang, Y.H., Kim, D.E., et al. (2015). Conductive fiber-based ultrasensitive textile pressure sensor for wearable electronics. Adv. Mater. *27*, 2433–2439. https://doi.org/10.1002/adma.201500009.

125. Zeng, W., Shu, L., Li, Q., Chen, S., Wang, F., and Tao, X.M. (2014). Fiber-based wearable electronics: a review of materials, fabrication, devices, and applications. Adv. Mater. *26*, 5310–5336. https://doi.org/10.1002/adma.201400633.

126. Kwak, M.K., Jeong, H.E., and Suh, K.Y. (2011). Rational design and enhanced biocompatibility of a dry adhesive medical skin patch. Adv. Mater. *23*, 3949–3953. https://doi.org/10.1002/adma.201101694.

127. Wang, L., Ha, K., Rodin, G., Liechti, K., and Lu, N. (2020). Mechanics of crater-enabled soft dry adhesives: a review. Front. Mech. Eng. *6*, 601510. https://doi.org/10.3389/fmech.2020.601510.

128. Choi, M.K., Park, O.K., Choi, C., Qiao, S., Ghaffari, R., Kim, J., Lee, D.J., Kim, M., Hyun, W., Kim, S.J., et al. (2016). Cephalopod-inspired miniaturized suction cups for smart medical skin. Adv. Healthc. Mater. *5*, 80–87. https://doi.org/10.1002/adhm.201500285.

129. Bartlett, M.D., Croll, A.B., King, D.R., Paret, B.M., Irschick, D.J., and Crosby, A.J. (2012). Looking beyond fibrillar features to scale gecko-like adhesion. Adv. Mater. *24*, 1078–1083. https://doi.org/10.1002/adma.201104191.

130. Bartlett, M.D., and Crosby, A.J. (2014). High capacity, easy release adhesives from renewable materials. Adv. Mater. *26*, 3405–3409. https://doi.org/10.1002/adma.201305593.

131. Baik, S., Lee, H.J., Kim, D.W., Kim, J.W., Lee, Y., and Pang, C. (2019). Bioinspired adhesive architectures: from skin patch to integrated bioelectronics. Adv. Mater. *31*, e1803309. https://doi.org/10.1002/adma.201803309.

132. Kim, T., Park, J., Sohn, J., Cho, D., and Jeon, S. (2016). Bioinspired, highly stretchable, and conductive dry adhesives based on 1D–2D hybrid carbon nanocomposites for all-in-one ECG electrodes. ACS Nano *10*, 4770–4778. https://doi.org/10.1021/acsnano.6b01355.

133. O'Rorke, R.D., Steele, T.W., and Taylor, H. (2016). Bioinspired fibrillar adhesives: a review of analytical models and experimental evidence for adhesion enhancement by surface patterns. J. Adhes. Sci. Technol. *30*, 362–391. https://doi.org/10.1080/01694243.2015.1101183.

134. Spolenak, R., Gorb, S., Gao, H., and Arzt, E. (2005). Effects of contact shape on the scaling of biological attachments. Proc. R. Soc. A: Math. Phys. Eng. Sci. *461*, 305–319. https://doi.org/10.1098/rspa.2004.1326.

135. Cadirov, N., Booth, J.A., Turner, K.L., and Israelachvili, J.N. (2017). Influence of humidity on grip and release adhesion mechanisms for gecko-inspired microfibrillar surfaces. ACS Appl. Mater. Inter. *9*, 14497–14505. https://doi.org/10.1021/acsami.7b01624.

136. Qiao, S., Wang, L., Jeong, H., Rodin, G.J., and Lu, N. (2017). Suction effects in cratered surfaces. J. R. Soc. Interf. *14*, 20170377. https://doi.org/10.1098/rsif.2017.0377.

137. Wang, L., Ha, K.-H., Qiao, S., and Lu, N. (2019). Suction effects of crater arrays. Extreme Mech. Lett. *30*, 100496. https://doi.org/10.1016/j.eml.2019.100496.

138. Chun, S., Kim, D.W., Baik, S., Lee, H.J., Lee, J.H., Bhang, S.H., and Pang, C. (2018). Conductive and stretchable adhesive electronics with miniaturized octopus-like suckers against dry/wet skin for biosignal monitoring. Adv. Funct. Mater. *28*, 1805224. https://doi.org/10.1002/adfm.201805224.

139. Baik, S., Kim, J., Lee, H.J., Lee, T.H., and Pang, C. (2018). Highly adaptable and biocompatible octopus-like adhesive patches with meniscus-controlled unfoldable 3D microtips for underwater surface and hairy skin. Adv. Sci. (Weinh) *5*, 1800100. https://doi.org/10.1002/advs.201800100.

140. Yang, S.Y., O'Cearbhaill, E.D., Sisk, G.C., Park, K.M., Cho, W.K., Villiger, M., Bouma, B.E., Pomahac, B., and Karp, J.M. (2013). A bio-inspired swellable microneedle adhesive for

mechanical interlocking with tissue. Nat. Commun. *4*, 1702. https://doi.org/10.1038/ncomms2715.

141. Seong, K.Y., Seo, M.S., Hwang, D.Y., O'Cearbhaill, E.D., Sreenan, S., Karp, J.M., and Yang, S.Y. (2017). A self-adherent, bullet-shaped microneedle patch for controlled transdermal delivery of insulin. J. Control. Release *265*, 48–56. https://doi.org/10.1016/j.jconrel.2017.03.041.

142. Yamagishi, K., Kirino, I., Takahashi, I., Amano, H., Takeoka, S., Morimoto, Y., and Fujie, T. (2019). Tissue-adhesive wirelessly powered optoelectronic device for metronomic photodynamic cancer therapy. Nat. Biomed. Eng. *3*, 27–36. https://doi.org/10.1038/s41551-018-0261-7.

143. Xiong, Y., Zhang, X., Ma, X., Wang, W., Yan, F., Zhao, X., Chu, X., Xu, W., and Sun, C. (2021). A review of the properties and applications of bioadhesive hydrogels. Polym. Chem. *12*, 3721–3739. https://doi.org/10.1039/D1PY00282A.

144. Pei, X., Wang, J., Cong, Y., and Fu, J. (2021). Recent progress in polymer hydrogel bioadhesives. J. Polym. Sci. *59*, 1312–1337. https://doi.org/10.1002/pol.20210249.

145. Xue, Y., Zhang, J., Chen, X., Zhang, J., Chen, G., Zhang, K., Lin, J., Guo, C., and Liu, J. (2021). Trigger-detachable hydrogel adhesives for bioelectronic interfaces. Adv. Funct. Mater. 2106446. https://doi.org/10.1002/adfm.202106446.

146. Mao, X., Yuk, H., and Zhao, X. (2020). Hydration and swelling of dry polymers for wet adhesion. J. Mech. Phys. Sol. *137*, 103863. https://doi.org/10.1016/j.jmps.2020.103863.

147. Chen, X., Yuk, H., Wu, J., Nabzdyk, C.S., and Zhao, X. (2020). Instant tough bioadhesive with triggerable benign detachment. Proc. Natl. Acad. Sci. U S A *117*, 15497–15503. https://doi.org/10.1073/pnas.2006389117.

148. Yamagishi, K., Zhou, W., Ching, T., Huang, S.Y., and Hashimoto, M. (2021). Ultra-deformable and tissue-adhesive liquid metal antennas with high wireless powering efficiency. Adv. Mater. *33*, e2008062. https://doi.org/10.1002/adma.202008062.

149. Meitl, M.A., Zhu, Z.-T., Kumar, V., Lee, K.J., Feng, X., Huang, Y.Y., Adesida, I., Nuzzo, R.G., and Rogers, J.A. (2006). Transfer printing by kinetic control of adhesion to an elastomeric stamp. Nat. Mater. *5*, 33–38. https://doi.org/10.1038/nmat1532.

150. Yeo, W.H., Kim, Y.S., Lee, J., Ameen, A., Shi, L., Li, M., Wang, S., Ma, R., Jin, S.H., Kang, Z., et al. (2013). Multifunctional epidermal electronics printed directly onto the skin. Adv. Mater. *25*, 2773–2778. https://doi.org/10.1002/adma.201204426.

151. Fang, Y., Li, Y., Li, Y., Ding, M., Xie, J., and Hu, B. (2020). Solution-processed submicron free-standing, conformal, transparent, breathable epidermal electrodes. ACS Appl. Mater. Inter. *12*, 23689–23696. https://doi.org/10.1021/acsami.0c04134.

152. Greco, F., Zucca, A., Taccola, S., Menciassi, A., Fujie, T., Haniuda, H., Takeoka, S., Dario, P., and Mattoli, V. (2011). Ultra-thin conductive free-standing PEDOT/PSS nanofilms. Soft Matter *7*, 10642–10650. https://doi.org/10.1039/C1SM06174G.

153. Kim, D.H., Lu, N., Ghaffari, R., Kim, Y.S., Lee, S.P., Xu, L., Wu, J., Kim, R.H., Song, J., Liu, Z., et al. (2011). Materials for multifunctional balloon catheters with capabilities in cardiac electrophysiological mapping and ablation therapy. Nat. Mater. *10*, 316–323. https://doi.org/10.1038/nmat2971.

154. Kim, M.S., Lee, G.J., Choi, C., Kim, M.S., Lee, M., Liu, S., Cho, K.W., Kim, H.M., Cho, H., Choi, M.K., et al. (2020). An aquatic-vision-inspired camera based on a monocentric lens and a silicon nanorod photodiode array. Nat. Electron. *3*, 546–553. https://doi.org/10.1038/s41928-020-0429-5.

155. Xie, K., and Wei, B. (2014). Materials and structures for stretchable energy storage and conversion devices. Adv. Mater. *26*, 3592–3617. https://doi.org/10.1002/adma.201305919.

156. Hure, J., Roman, B., and Bico, J. (2011). Wrapping an adhesive sphere with an elastic sheet. Phys. Rev. Lett. *106*, 174301. https://doi.org/10.1103/PhysRevLett.106.174301.

157. Lee, Y.K., Xi, Z., Lee, Y.J., Kim, Y.H., Hao, Y., Choi, H., Lee, M.G., Joo, Y.C., Kim, C., Lien, J.M., et al. (2020). Computational wrapping: a universal method to wrap 3D-curved surfaces with nonstretchable materials for conformal devices. Sci. Adv. *6*, eaax6212. https://doi.org/10.1126/sciadv.aax6212.

158. Williams, N.X., Noyce, S., Cardenas, J.A., Catenacci, M., Wiley, B.J., and Franklin, A.D. (2019). Silver nanowire inks for direct-write electronic tattoo applications. Nanoscale *11*, 14294–14302. https://doi.org/10.1039/c9nr03378e.

159. Zhu, Z., Guo, S.Z., Hirdler, T., Eide, C., Fan, X., Tolar, J., and McAlpine, M.C. (2018). 3D printed functional and biological materials on moving freeform surfaces. Adv. Mater. *30*, e1707495. https://doi.org/10.1002/adma.201707495.

160. Choi, Y., .Ryu, N., .Kim, M.J., .Dementyev, A., and .Bianchi, A., eds. BodyPrinter: fabricating circuits directly on the skin at arbitrary locations using a wearable compact plotter. In Proceedings of the 33rd Annual ACM Symposium on User Interface Software and Technology (Association for Computing Machinery), pp. 554–564.

161. Fan, Y.J., Li, X., Kuang, S.Y., Zhang, L., Chen, Y.H., Liu, L., Zhang, K., Ma, S.W., Liang, F., Wu, T., et al. (2018). Highly robust, transparent, and breathable epidermal electrode. ACS Nano *12*, 9326–9332. https://doi.org/10.1021/acsnano.8b04245.

162. Chen, Y., Lu, B., Chen, Y., and Feng, X. (2015). Breathable and stretchable temperature sensors inspired by skin. Sci. Rep. *5*, 11505. https://doi.org/10.1038/srep11505.

163. Zhou, W., Yao, S., Wang, H., Du, Q., Ma, Y., and Zhu, Y. (2020). Gas-permeable, ultrathin, stretchable epidermal electronics with porous electrodes. ACS Nano *14*, 5798–5805. https://doi.org/10.1021/acsnano.0c00906.

164. Huang, Z., Hao, Y., Li, Y., Hu, H., Wang, C., Nomoto, A., Pan, T., Gu, Y., Chen, Y., Zhang, T., et al. (2018). Three-dimensional integrated stretchable electronics. Nat. Electron. *1*, 473–480. https://doi.org/10.1038/s41928-018-0116-y.

165. Kang, J., Son, D., Vardoulis, O., Mun, J., Matsuhisa, N., Kim, Y., Kim, J., Tok, J.B.H., and Bao, Z. (2019). Modular and reconfigurable stretchable electronic systems. Adv. Mater. Tech. *4*, 1800417. https://doi.org/10.1002/admt.201800417.

166. Shi, C., Zou, Z., Lei, Z., Zhu, P., Zhang, W., and Xiao, J. (2020). Heterogeneous integration of rigid, soft, and liquid materials for self-healable, recyclable, and reconfigurable wearable electronics. Sci. Adv. *6*, eabd0202. https://doi.org/10.1126/sciadv.abd0202.

167. Brown, P. (2018). FLEX 2018: flexible arduino? Flexible hybrid electronics reaches a new milestone. https://electronics360.globalspec.com/article/11153/flex-2018-flexible-arduino-flexible-hybrid-electronics-reaches-a-new-milestone.

168. Jang, K.I., Han, S.Y., Xu, S., Mathewson, K.E., Zhang, Y., Jeong, J.W., Kim, G.T., Webb, R.C., Lee, J.W., Dawidczyk, T.J., et al. (2014). Rugged and breathable forms of stretchable electronics with adherent composite substrates for transcutaneous monitoring. Nat. Commun. *5*, 4779. https://doi.org/10.1038/ncomms5779.

169. Yeon, H., Lee, H., Kim, Y., Lee, D., Lee, Y., Lee, J.-S., Shin, J., Choi, C., Kang, J.-H., Suh, J.M., et al. (2021). Long-term reliable physical health monitoring by sweat pore–inspired perforated electronic skins. Sci. Adv. *7*, eabg8459. https://doi.org/10.1126/sciadv.abg8459.

170. Shu, L., Xu, T., and Xu, X. (2019). Multilayer sweat-absorbable textile electrode for EEG measurement in forehead site. IEEE Sensor. J. *19*, 5995–6005. https://doi.org/10.1109/JSEN.2019.2912667.

171. Heikenfeld, J. (2016). Bioanalytical devices: technological leap for sweat sensing. Nature *529*, 475–476. https://doi.org/10.1038/529475a.

172. Koh, A., Kang, D., Xue, Y., Lee, S., Pielak, R.M., Kim, J., Hwang, T., Min, S., Banks, A., Bastien, P., et al. (2016). A soft, wearable microfluidic device for the capture, storage, and colorimetric sensing of sweat. Sci. Transl. Med. *8*, 366ra165. https://doi.org/10.1126/scitranslmed.aaf2593.

173. Rose, D.P., Ratterman, M.E., Griffin, D.K., Hou, L., Kelley-Loughnane, N., Naik, R.R., Hagen, J.A., Papautsky, I., and Heikenfeld, J.C. (2015). Adhesive RFID sensor patch for monitoring of sweat electrolytes. IEEE Trans. Biomed. Eng. *62*, 1457–1465. https://doi.org/10.1109/TBME.2014.2369991.

174. Liu, J., Fu, T.M., Cheng, Z., Hong, G., Zhou, T., Jin, L., Duvvuri, M., Jiang, Z., Kruskal, P., Xie, C., et al. (2015). Syringe-injectable electronics. Nat. Nanotechnol. *10*, 629–636. https://doi.org/10.1038/nnano.2015.115.

175. Li, Q., Nan, K., Le Floch, P., Lin, Z., Sheng, H., Blum, T.S., and Liu, J. (2019). Cyborg organoids: implantation of nanoelectronics via organogenesis for

tissue-wide electrophysiology. Nano Lett. *19*, 5781–5789. https://doi.org/10.1021/acs.nanolett.9b02512.

176. Koo, J.H., Song, J.K., Yoo, S., Sunwoo, S.H., Son, D., and Kim, D.H. (2020). Unconventional device and material approaches for monolithic biointegration of implantable sensors and wearable electronics. Adv. Mater. Tech. *5*, 2000407. https://doi.org/10.1002/admt.202000407.

177. Choi, Y., Koo, J., and Rogers, J.A. (2020). Inorganic materials for transient electronics in biomedical applications. MRS Bull. *45*, 103–112. https://doi.org/10.1557/mrs.2020.25.

178. Tan, M.J., Owh, C., Chee, P.L., Kyaw, A.K.K., Kai, D., and Loh, X.J. (2016). Biodegradable electronics: cornerstone for sustainable electronics and transient applications. J. Mater. Chem. C *4*, 5531–5558. https://doi.org/10.1039/C6TC00678G.

179. Yu, X., Shou, W., Mahajan, B.K., Huang, X., and Pan, H. (2018). Materials, processes, and facile manufacturing for bioresorbable electronics: a review. Adv. Mater. *30*, e1707624. https://doi.org/10.1002/adma.201707624.

180. Yang, J.C., Mun, J., Kwon, S.Y., Park, S., Bao, Z., and Park, S. (2019). Electronic skin: recent progress and future prospects for skin-attachable devices for health monitoring, robotics, and prosthetics. Adv. Mater. *31*, e1904765. https://doi.org/10.1002/adma.201904765.

181. Onuki, Y., Bhardwaj, U., Papadimitrakopoulos, F., and Burgess, D.J. (2008). A review of the biocompatibility of implantable devices: current challenges to overcome foreign body response. J. Diabetes Sci. Technol. *2*, 1003–1015. https://doi.org/10.1177/193229680800200610.